Available online at www.sciencedirect.com

ScienceDirect

Coordination Chemistry Reviews 251 (2007) 2400–2427

COORDINATION CHEMISTRY REVIEWS

www.elsevier.com/locate/ccr

Review

Mercury alkynyls as versatile templates for new organometallic materials and polymers

Wai-Yeung Wong [*]

Department of Chemistry and Centre for Advanced Luminescence Materials, Hong Kong Baptist University, Waterloo Road, Kowloon Tong, Hong Kong, PR China

Received 25 October 2006; accepted 22 January 2007
Available online 25 January 2007

Contents

Abstract

Rigid-rod transition metal alkynyl compounds of various group 10 and 11 elements have been widely studied over the past decades in different domains of material science because of their unique structures and photophysical properties. However, the designed synthesis and thorough investigation of the parallel chemistry of group 12 mercury alkynyl compounds has been relatively under explored. This article summarizes recent progress in the developments of linear mercury-based metallaynes as well as their long-chain oligomers and polymers. These novel organomercurial materials exhibit interesting chemical, physical and material properties. Synthetic avenues towards the preparation of these mercury(II) alkynyl compounds and their photophysical and solid-state structural features are comprehensively reviewed. Practical utilization of these mercury alkynyls in different areas including optoelectronic and analytical applications are critically discussed in this review. The future developments of this research frontier are also envisaged.

Keywords: Alkynyl; Crystal structures; Luminescence; Mercury; Mercurophilicity; Metallopolymers

---

Abbreviations: ^{n}Bu, *n*-butyl; CIS, singles configuration interaction; CVAFS, cold vapor atomic fluorescence spectroscopy; Cy, cyclohexyl; DFT, density functional theory; DP, degree of polymerization; dppe, bis(diphenylphosphino)ethane; dppm, bis(diphenylphosphino)methane; DSC, differential scanning calorimetry; ECD, electron capture detector; EH, extended Hückel; Et, ethyl; FAB, fast-atom bombardment; Fc, ferrocenyl group (η^5-C_5H_5)(η^5-C_5H_4)Fe; GC, gas chromatography; GPC, gel permeation chromatography; HOMO, highest occupied molecular orbitals; HPLC, high-performance liquid chromatography; IE, ionization energy; IR, infrared; ISC, intersystem crossing; $(k_{nr})_P$, nonradiative phosphorescence decay rate constant; $(k_r)_P$, radiative phosphorescence decay rate constant; LED, light-emitting diodes; LLCT, ligand–ligand charge transfer; LUMO, lowest unoccupied molecular orbitals; Me, methyl; MLCT, metal to ligand charge transfer; MS, mass spectrometry; M_n, number-average molecular weights; M_W, weight-average molecular weights; OAc, acetate; OPL, optical power limiting; NMR, nuclear magnetic resonance; Ph, phenyl; phen, 1,10-phenanthroline; PL, photoluminescence; PPE, poly(*p*-phenyleneethynylene)s; ^{n}Pr, *n*-propyl; S_1, first singlet excited state; pz, pyrazol-1-yl; *T*, transmittance; T_1, first triplet excited state; TDDFT, time-dependent density functional theory; TGA, thermogravimetric analysis; Tol, tolyl; UV–vis, ultraviolet–visible; VDW, van der Waals

[*] Tel.: +852 34117074; fax: +852 34117348.
E-mail address: rwywong@hkbu.edu.hk.

doi:10.1016/j.ccr.2007.01.006

1. Introduction and scope of this review

Since the synthesis of polyynes containing transition metals of group 10 in the main chain by Sonogashira and co-workers [1–4], the chemistry of metal acetylides has become the focus of enormous attention with the emerging interest in their potential applications in the field of materials science [5–12]. The general structure for the prototype polymetallayne is shown in Fig. 1, in which the polymer has a linear backbone with the metal center M, the spacer group R and the auxiliary ligand L on the metal center. Recently, different synthetic approaches have been developed, extending the data covering the polymeric species and their corresponding oligomeric forms for group 8–11 transition metals and for a large class of π-conjugated bridging ligands [13–21]. Because of the introduction of the metal–ligand groups, $M(L)_n$, into the polyyne backbone, these materials offer versatility that cannot be matched by the conventional π-conjugated organic polymers such as polythiophene and polyacetylene. For instance, changing the nature of the ligands may improve the solubility of the polymer without significantly altering the electrical properties, which are principally derived from the π-system of the hydrocarbon backbone. Such research endeavor provides a good opportunity for coupling the chemical, electronic and optical properties of metal complexes to those of the organic chromophoric component, thus accessing novel metal-based polymers with new functional properties [22].

The d^{10} gold(I) and mercury(II) centers are isolobal and isoelectronic to each other. Although the organometallic chemistry of the group 11 metals with σ-alkynyl ligands to produce luminescent complexes dates back almost four decades ago [23–25], over the years, interest in the study of mono-, di- and polynuclear gold(I) σ-acetylide complexes has stemmed not only from their rich photochemistry but also from the observation of weak intermolecular d^{10}–d^{10} Au···Au interactions which can play an important role in materials science and crystal engineering [26–33]. In many cases, it is the combination of the complementary intermolecular forces of aurophilic interactions, hydrogen bonding, π–π stacking and other non-covalent interactions that determines the solid-state luminescent properties of these organometallic materials. Linear two-coordinate gold(I) complexes of the type $[AuX_2]^-$ (X = substituted alkynyl group) have potential as building blocks for supramolecular structures because of their relatively simple molecular geometry. Moreover, there is evidence for ready association of these species into dimers, oligomers, and polymers as a result of attractive intermolecular Au···Au interactions [34,35]. The strengths of the gold–gold interactions are comparable with those found in hydrogen bonds [36,37] and they seem to be responsible for the intriguing optical properties of some of these compounds [38]. For example, formation of Au···Au and aryl–aryl interactions in the solid state can cause a red-shift in the emission band compared with that in the solution phase [39,40]. In contrast to the vast body of work on alkynylgold(I) compounds, the chemistry of metal-alkynyls of the neighboring group 12 elements, especially the d^{10} mercury(II)-alkynyl compounds is still relatively under explored. In view of this clear deficiency, and the recent renaissance in the mercurophilicity phenomenon exhibited by organomercurials, we and others have been actively engaged in a project aiming at synthesizing some Hg(II) alkynyl molecular systems that have a close analogy to those for other known transition metals.

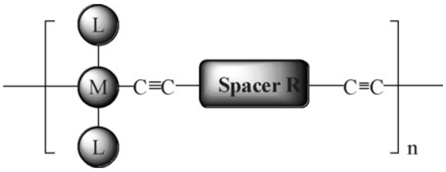

Fig. 1. General structure of metallopolyyne.

Although mercury(II) acetylides were known as early as 1920s [41], they are limited to those of simple alkyl- and arylmercury derivatives. These species can be utilized for their luminescence, but more importantly as ligand-transfer reagents [42,43]. Considerable efforts have been devoted to extending the work to various polymeric and supramolecular assemblies [44,45]. The linear geometry of the alkynyl unit and its π-unsaturated character have led to mercury(II) alkynyls becoming attractive building blocks for molecular wires and organometallic functional materials, which possess interesting properties such as optical nonlinearity, luminescence and chemosensing and mercurophilicity (Fig. 2). Herein, a survey of various alkynyl complexes of mercury(II) is given and as far as we are aware, this is the first article to review solely the synthesis of mercury alkynyl complexes and polymers, their structural diversity, and their potential application in a wide domains of materials science research. The many examples covered in this contribution highlight the richness and diversity in such a research scenario.

2. Structure and bonding of mercury alkynyls

Zinc, cadmium and mercury follow copper, silver and gold in the periods 4–6 of the periodic table and have two s electrons outside filled d shells. The group 12 metal(II) ions contain d^{10} closed shell electron configuration. Due to the high ionization potentials (IE) of closed shell metal ions (e.g. IE = 40 eV for Zn(II) and 38 eV for Cd(II)), any states involving excitation of the d electron should have a high energy [46]. Therefore, d–d transitions are predominantly absent in group 12 complexes. Consequently, the lowest energy excited states for these complexes are essentially composed of ligand-centered and/or ligand–ligand charge-transfer (LLCT) states. Among the group 12 metals, cadmium is chemically very like zinc and any differences are attributable to the larger sizes of the Cd atom and Cd^{2+} ion. Mercury is distinct and does bear some resemblance to Cd, but in many respects is very like Au and Tl. For Cd, the +2 oxidation state is of utmost importance, but compounds of Hg(I) and Hg(II) are both well known. Mercury is unique among the group 12 metals in forming a stable $[M_2]^{2+}$ ion. Like Cd^{2+}, Hg^{2+} is a soft metal center, and coordination to S-donors is most favored. Comparing the promotional energies for $ns^2 \rightarrow ns^1np^1$ (433, 408, and 524 kJ/mol for Zn, Cd, and Hg, respectively) involved in the formation of two covalent bonds for these three elements, further ligands cannot be added readily to metals,

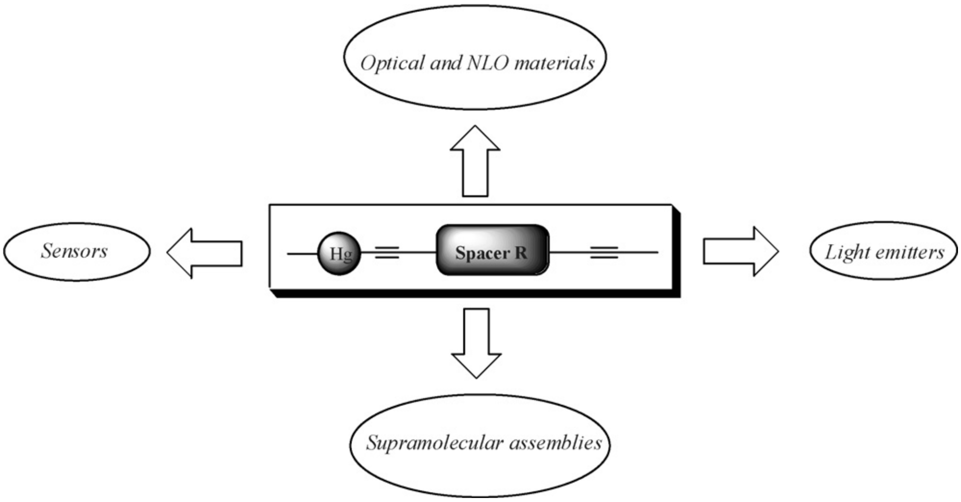

Fig. 2. Applications of alkynylmercury(II) compounds in materials science.

particularly for Hg. This is probably the main reason that two-coordination is the commonest for Hg. Mercury(II) ion has a rich but rather simple coordination chemistry and can afford a variety of complexes with organic and inorganic ligands by forming mostly two-coordinate d^{10} mercury(II) species [47]. The Hg^{2+} ion has indeed a strong tendency to complex formation, and the most stable complexes are those with C, N, P, and S as ligand atoms. Indeed, linear two-coordination is more characteristic for Hg^{2+} than for any other metal species. While mercury(II) ion tends to possess a coordination number of two with linear stereochemistry, it is well suited for forming rigid-rod polymers. In mercury acetylide compounds and polymers, Hg atoms are bonded to acetylides by metal–carbon σ-bonds and polymers have a rigid-rod backbone based on the linear carbon–carbon triple bonds.

Transition metal alkynyl complexes can often be treated as complexes of the $HC{\equiv}C^-$ ligand, which is actually isoelectronic with CO, CN^- and N_2. The stoichiometry of these complexes is closely related to the corresponding cyanide complexes, and the alkynyl ligand can also be thought of as a pseudohalide because of its behavior in complex formation and precipitation reactions. Therefore, the chemistry of mercury alkynyl complexes belongs to a combined study of classical coordination and organometallic chemistry [48]. On the other hand, there is a simple frontier-orbital relationship between alkynyl and cyanide ligands, and from the wide-ranging spectroscopic and magnetic studies, the two ligands are shown to occupy similar strong-field positions in the spectrochemical series. There is still some debate as to whether the σ-alkynyl ligands act as π-donors through the π-bonding molecular orbitals of the triple bond or as π-acceptors. The level of π-donor or -acceptor contribution may change with the metal present, with the donor properties being more prominent for the earlier transition metals but the π-acceptor component being more important for the later metals such as mercury. The first direct evidence for the participation of mercury 5d-electrons in mercury–carbon bonding has been recently provided by He(I) and He(II) photoelectron spectroscopy of $Hg(C{\equiv}CR)_2$ ($R = CH_3, C_4H_9$, Cl) [49]. A number of theoretical and spectroscopic investigations have been performed to understand the nature of π-interactions in M–C≡C–R fragments and the role of alkynyl R groups. The vibrational modes of M–C, C≡C and C≡C–R bonds need to be assigned to study the metal-alkynyl bonding. In most instances, the C≡C bond stretch has a distinctive frequency range and is readily assigned [50].

This article reviews current research work carried out by us and others on alkynylmercury(II) complexes and their corresponding oligomers and polymers. The oligometallaynes can generally be considered as models and building blocks for the high-molecular-weight polymers and important information on their molecular and electronic properties can be obtained through the detailed studies of these model compounds. The organomercurial compounds to be discussed are classified according to the types of the chromophoric units. Herein, mononuclear, dinuclear and polynuclear metal alkynyl systems of mercury are discussed, and particular attention is focused on the electronic absorption spectroscopy and photoluminescence behavior, electronic structures, thermal stability and structural aspects of these mercury-containing metallaynes. All the metal polyynes and their molecular model compounds reported were characterized as fully as possible using conventional spectroscopic techniques. The role of intermolecular mercurophilic short contacts and practical utilization of these metallopolymers in different domains are critically discussed.

3. Survey of alkynylmercury complexes and polymers

Before the advent of modern spectroscopic methods for compound characterization, the conversion of an organic compound to a crystalline derivative was common practice. In the case of terminal alkynes, bis(alkynyl)mercurials $Hg(C{\equiv}CR)_2$ were often the derivative of choice. The conventional synthesis of mercury-alkynyl σ complexes is achieved either by the reaction of mercury halides with anionic alkynylating agents such as alkali-metal [51], magnesium [51,52] or copper alkynyl compounds [51,52], or alternatively by direct dehydrohalogenation protocol in the reaction between metal halides and active terminal alkynes in the presence of a base [53] (see Eqs. (1)–(3)). Reaction of $Hg(C{\equiv}CR)_2$ (R = alkyl or aryl group) with low-valent late transition metal centers may result in insertion of the metal into one Hg–C bond [54] or in some cases such a species may evolve elemental mercury, providing a catalytic process for the synthesis of symmetrical 1, 3-diynes [55,56]. Bis(alkynyl)mercurials react with some metal complexes to afford 1, 3-diynes via catalytic demercuration. In bi- and polynuclear systems, they have been shown to provide C≡CR, RC≡CC≡CR, or HgC≡CR fragments [57,58]. The mercury center displays weak Lewis acidity [59], such that in reactions with nucleophiles these reagents can effectively serve as electrophilic alkynyl equivalents, following mercury extrusion [60]. We have been inspired to focus on the various modern Hg–C≡C$^-$ σ-bond forming reactions, which are relevant not only for simple monomeric metal alkynyls, but also for their increasingly important oligomeric and polymeric analogues. Nevertheless, the characterization of mercury alkynyl complexes is problematic because of their insolubility in common organic solvents:

$$2R{-}C{\equiv}CH + K_2HgI_4 + 2KOH \rightarrow Hg(C{\equiv}C{-}R)_2 + 4KI + 2H_2O \qquad (1)$$

$$2R{-}C{\equiv}CM + HgCl_2 \rightarrow Hg(C{\equiv}C{-}R)_2 + 2MCl \qquad (2)$$

$$2R{-}C{\equiv}CH + HgCl_2 + 2NaOH \rightarrow Hg(C{\equiv}C{-}R)_2 + 2NaCl \qquad (3)$$

3.1. Compounds with hydrocarbyl, arylene and related groups

A large series of simple symmetric mercuric alkynyl compounds of the formula $Hg(C{\equiv}CR)_2$ have been prepared, in which the substituted R groups can be aliphatic, aromatic and mixed aromatic–aliphatic groups [41,61,62]. A list of compounds **1a**–**1r** together with their asymmetric monoalkynyl derivatives of the form $R'Hg(C{\equiv}CR)$ and dinuclear complexes $R'Hg{-}C{\equiv}C{-}HgR'$ were characterized by ^{1}H, ^{13}C and ^{199}Hg NMR techniques [63]. Infrared and Raman spectroscopies have been used to study the vibrational features of the complex $CH_3Hg{-}C{\equiv}CH$ [64]. Because of the isoelectronic relationship between the C≡CH group and CN$^-$ ligand, normal coordinate calculations were carried out to confirm the assignments and the larger force constant for the Hg–C≡CH fragment in $CH_3Hg{-}C{\equiv}CH$ (2.83 mdyn/Å) than that for the Hg–CN stretching in CH_3HgCN (2.13 mdyn/Å) suggests that the former bond is stronger than the latter. A similar approach was used to study the vibrational spectra of $CH_3Hg(C{\equiv}CCH_3)$ and its deuterated analogues in detail [65]. A strong IR absorption at ca. 2150 cm^{-1} in each isotopic species is found to be hardly affected by deuteration and the corresponding Raman spectral band in solution is polarized. This can be assigned to the C≡C stretching mode. Normal coordinate analyses again reveal that the force constants for the Hg–C≡C bond are always larger than those for the $Hg{-}CH_3$ bond. This is consistent with the expectation on the basis of the hybridization of the carbon atom adjacent to the metal atom and the sp hybridization in Hg–C≡C and the sp^3 hybrid in $Hg{-}CH_3$ make the former bond stronger than the latter.

Nicholson and co-workers have studied the solid-state aggregation phenomenon of two mercury bis(acetylides) **1h** and **1i** using X-ray crystallography in which weak Hg···Hg short contacts were observed and the main driving force for molecular clustering appears to be the interactions between Hg atoms and the C≡C bonds of adjacent molecules (vide infra) [66].

$R{-}C{\equiv}C{-}Hg{-}C{\equiv}C{-}R$

1

R= $-Cl$ **a**, $-Br$ **b** , $-CH_3$ **c**, $-C_2H_5$ **d**, $-C_4H_7$ **e**, $-C_5H_{11}$ **f**, $-C_8H_{17}$ **g**, $-SiMe_3$ **h**

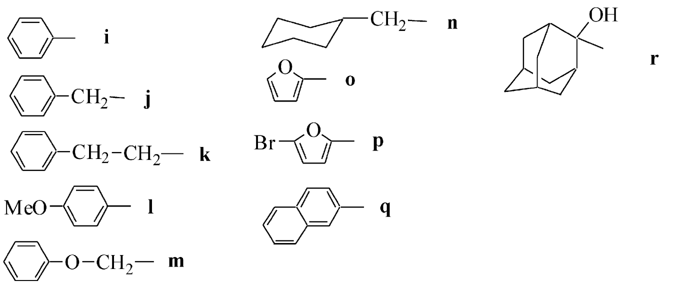

Alkynyl ligand transfer reactions based on $Hg(C{\equiv}CR)_2$ are also common for making some transition metal and rare earth complexes. For instance, $Hg(C{\equiv}CPh)_2$ was found to trigger the ethynyl transfer between platinum and mercury according to the Eq. (4) [67]. The mixed-metal platinum-mercury alkynyls $[(RC{\equiv}C)_2Pt(\mu\text{-dppm})_2HgCl_2]$ can be obtained in high yields from the fast reaction between $[Pt(dppm\text{-}PP')_2]Cl_2$ and $Hg(C{\equiv}CR)_2$ (R = Ph, Tol, Me, ^{n}Pr) [68]. Recently, HgPh(C≡CPh) was used for the synthesis of some novel organolanthanoids containing bridging C≡CPh ligands between two lanthanide metal ions [69]:

$$cis\text{-}[PtCl_2(PMePh_2)] + 2Hg(C{\equiv}CPh)_2 \rightarrow trans\text{-}[Pt(C{\equiv}CPh)_2(PMePh_2)_2] + 2HgCl(C{\equiv}CPh) \qquad (4)$$

Trifluoropropynyllithium reagent was prepared by a novel one-pot procedure from 1,1,1,3,3-pentafluoropropane which can be employed to afford $Hg(C{\equiv}CCF_3)_2$ in moderate yield [70]. Two trifluoropropynylmercury complexes $RHg(C{\equiv}CCF_3)$ (R = Ph, Fc) have been reported which represent two of the very few structurally characterized examples of fluorinated alkynylmercurial species in the literature other than the earlier reported $Hg(C{\equiv}CCF_3)_2$ [71]. Both of them exhibited the presence of appreciable mercury-centered intermolecular interactions in the extended structures showing Hg···Hg and Hg···η^2-C≡C short contacts. However, it is worth noting that there are potential explosive hazards for using a large amount of $Hg(C{\equiv}C^{i}Pr)_2$ and $Hg(C{\equiv}CFc)_2$ [72]. These complexes crystallize with mercurophilic interactions that bring adjacent alkynyl groups within close proximity. A phase change upon warming may thus result in a large pressure to cause explosive demercuration.

Several fluorescent-labelled methylmercury acetylides **2**–**4** were reported by Bolletta et al. in which anthracene, acridone and dansyl chromophores were anchored to the metal core by simple alkynlation [73]. There is no big differences in the absorption and emission spectra between uncomplexed and complexed species in all three cases. The authors also claimed that the uncomplexed fluorescent labels can be exploited for the HPLC analysis of methylmercury.

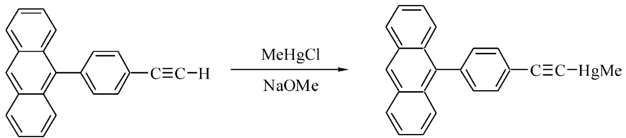

2

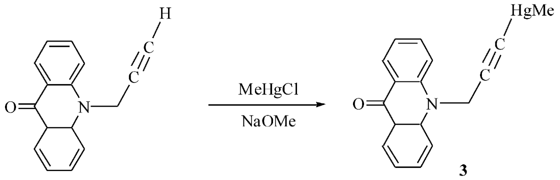

3

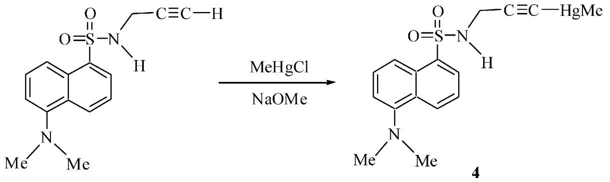

4

Two mercury alkynyl complexes derived from 4-ethynylpyridine (**5**) and (4-ethynylphenyl)(4-pyridyl)acetylene (**6**) were isolated in 62–65% which were fully characterized by IR and NMR spectroscopies and mass spectrometry [74,75]. The X-ray structure of **5** was established which reveals infinite zigzag chains of molecular entities showing a T-shaped coordination geometry in the lattice [74]. The photophysical properties and the ability for forming self-assembled molecular polygons based on **5** and **6** were compared to those for the corresponding anionic gold(I) counterparts. These compounds may serve as versatile building units for affording new metallosupramolecular systems [75]. With bidentate imine ligands such as 1,10-phenanthroline (phen), Hg(C≡CPh)$_2$ forms a 1:1 adduct with phen to give **7** whose structure was confirmed by X-ray analysis [76]. The Hg atom is four-coordinate with a mean Hg–N distance of 2.68 Å and the C≡C bond length appears unaffected by metal coordination. The crystal structure of **8** was also determined [77].

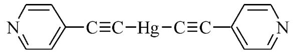

5

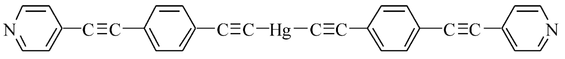

6

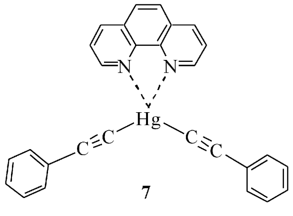

7

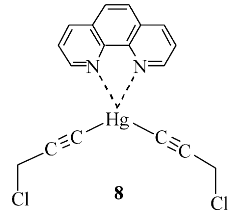

8

The classical work has successfully been extended to the dinuclear and polynuclear systems and compounds **9** and **10** spaced by biphenyl rings were recently prepared [78]. Only the lower-molecular-weight fraction of **10** can readily dissolve in organic solvents and there is always some insoluble portion left in the polymer solution. The crystal structure of **9** was determined providing conclusive proof of the linear two-coordinate configuration at mercury (vide infra). The polymeric mercury(II) acetylide system is aggregated in the solid state through extensive Hg· · ·Hg secondary interactions, which are also reflected by the presence of a broad aggregate band in its photoluminescence (PL) spectrum (Fig. 3). The spatial extent of the lowest singlet (S_1) and triplet (T_1) excited states with chain length was examined for **9** and **10** and the S_1–T_1 energy gap of 0.70–0.76 eV was observed. The results were also correlated to those triplet-emitting compounds harnessed through the heavy platinum and gold centers. The electronic structure of the Hg polyyne **10** was also investigated using extended Hückel (EH) theory and compared to other metal oligoyne polymers of the nearest metal neighbors [79].

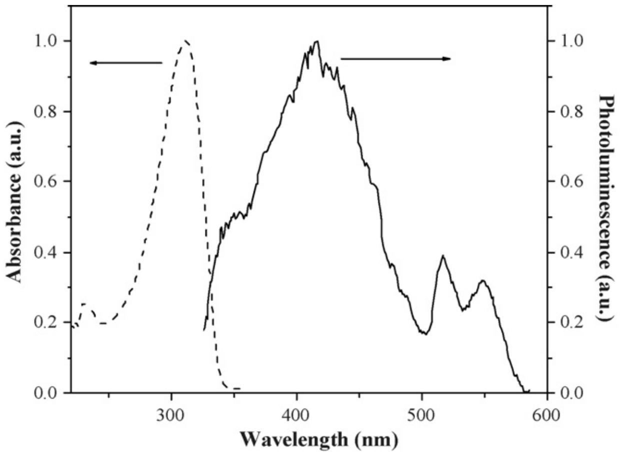

Fig. 3. Absorption (298 K) and PL (77 K) spectra of **10** in CH_2Cl_2 [78].

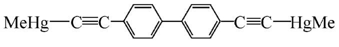

9

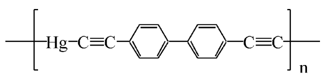

10

In a related context, Gabbaï et al. studied the supramolecular adduct formation of [o-C_6F_4Hg]$_3$ with a series of α,ω-diphenylpolyynes via weak but extensive secondary Hg–π interactions [80]. These adducts were fully characterized by a combination of elemental analysis, X-ray crystallography, IR and emission spectroscopy, DSC and TGA. Such an approach was shown to be interesting for the stabilization of these otherwise highly reactive hydrocarbon-based alkynes without much affecting the structure of the parent polyynes.

The first example of a trinuclear mercury(II) triacetylide complex of 1,3,5-triethynylbenzene **11** was described recently, from which we have been able to study its spectroscopic and luminescent properties and the results were compared with the isolobal gold(I) congener [{(PPh$_3$)AuC≡C}$_3$(1,3,5-C_6H_3)] [81]. From the absorption data, the π-delocalization through the metal chromophore is better for Au(I) than Hg(II). Our investigations indicate that the organic triplet emissions can be harvested by the heavy-atom effect of mercury which enables efficient intersystem crossing from the S_1 state to the T_1 state. The influence of Hg and Au centers on the phosphorescence efficiency and evolution of the lowest electronic S_1 and T_1 excited states is critically characterized. Both Hg and Au complexes possess high-energy triplet states of 2.77–2.82 eV, and the order of intersystem crossing (ISC) rate follows the order Au > Hg.

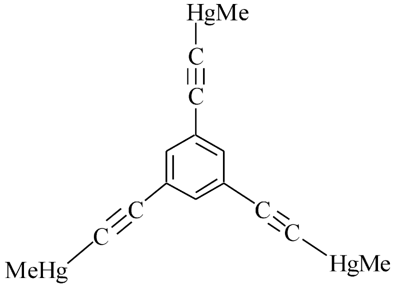

11

Two dialkoxy-substituted mercury-containing poly(*p*-phenyleneethynylene) (PPE) copolymers **12** and **13** were also prepared, both of which feature long-alkyl chains on the phenylene rings to make the polymers more organic-soluble [82]. Both organomercurial polymers possess high molecular weights of 35,630–44,760 (DP = 75 for **12** and 44 for **13**). They were found to exhibit slightly different thermal and PL properties with respect to the relative positions of the substituent groups.

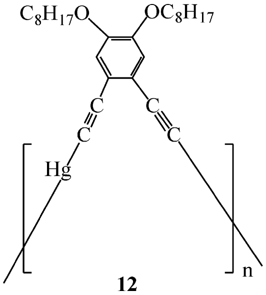

12

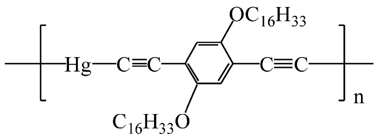

13

A novel approach based on π-conjugation interruption was developed recently by us for a series of luminescent and thermally stable group 16 chalcogen-bridged mercury(II) diyne complexes **14**–**17** and polyyne polymers **18**–**21** in which the conjugation path is limited by the presence of an insulating spacer [83]. The feed mole ratios of the mercury(II) chloride precursors and the diethynyl ligands were 2:1 and 1:1 for the diyne and polyyne syntheses, respectively. However, attempts to make the polyynes **18**–**21** only resulted in insoluble substances but IR studies confirmed the formation of rigid-rod Hg polyynes. An in-depth investigation of the photophysical properties of these group 12 metallayne materials was made and important correlations were drawn relative to their group 10 diplatinum and group 11 digold closest neighbors. The regiochemical structures of these angular-shaped molecules were studied by NMR spectroscopy and single-crystal X-ray structural analyses (vide infra). Harvesting of organic triplet emissions harnessed through the heavy-atom effects of group 10–12 transition metals was systematically probed (Fig. 4). Compounds **14**–**17** were found to have large optical gaps and high-energy T_1 states. The influence of Hg and chalcogen-based conjugation-interruptors on the intersystem crossing rate and the evolution of the lowest singlet and triplet excitons was fully elucidated (Fig. 5). The dependence of the S_1 and T_1 electronic states on the electronic structure of the chalcogen spacer groups was examined in detail. Generally, the order of triplet energies is $O > SO_2 > SO > S$ for **14**–**17**, but the phosphorescent yield is relatively insensitive to the nature of the chalcogen group. While it appears that chalcogenide centers do not show coordinating ability, they play more than a spectator's role in being a good conjugation-interruptor. The results are remarkable in regard to achieving comparable orders of magnitude for $(k_{nr})_P$ and $(k_r)_P$ which are rarely the case

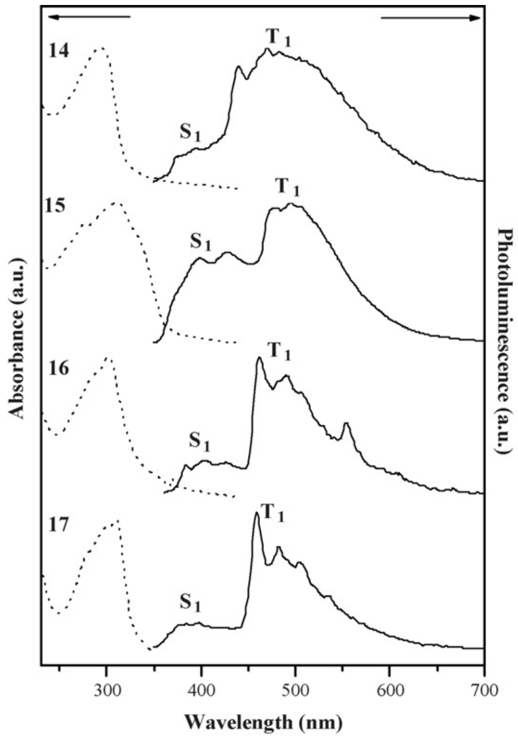

Fig. 4. Phosphorescence spectra of **14**–**17** at 11 K [83].

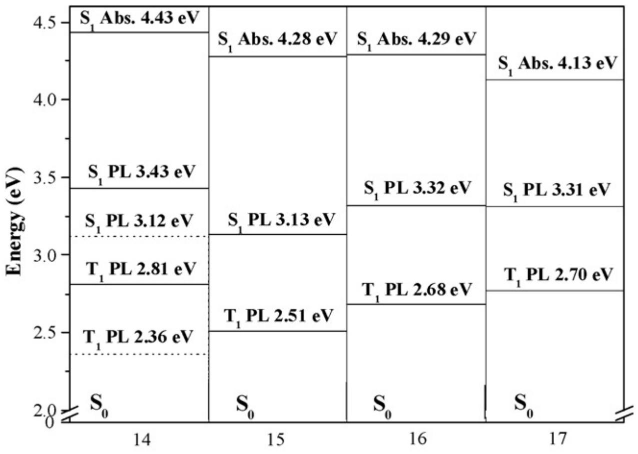

Fig. 5. Energy level diagram for **14**–**17**. The levels for **9** are shown as dashed lines in the left column [83].

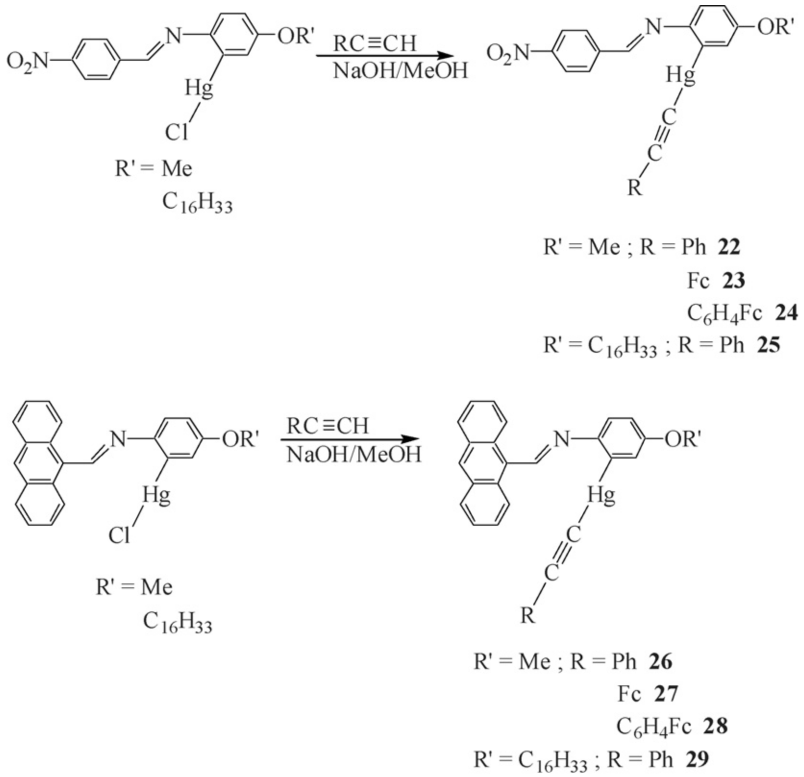

Fig. 6. Synthesis of **22–29** [84].

for polymetallaynes containing π-conjugated spacers (Fig. 6).

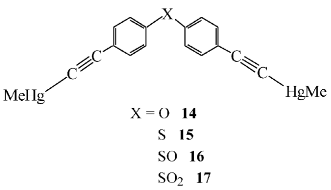

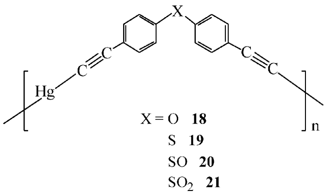

A novel series of σ-alkynyl complexes of orthomercurated Schiff bases of substituted benzylideneanilines **22–25** and anthracenylmethyleneanilines **26–29** were synthesized in good yield from alkynylation of the mercuric chlorides of the appropriate Schiff bases with some terminal alkynes RC≡CH (R = Ph, Fc, *p*-ferrocenylphenyl) at room temperature under basic medium [84]. All the new compounds generally displayed good solubility in polar organic solvents and their identities were completely elucidated by various spectroscopic methods. The solid-state structures of these compounds suggest that the alkynylmercury(II) moiety is directed to the *ortho* position of the *N*-phenyl ring of the Schiff bases. Depending on the geometric and steric properties of the end groups anchored on the alkynyl unit and the type of Schiff base employed, we can get polymeric mercury(II) alkynyl systems in the solid state aggregated through Hg· · ·Hg and Hg· · ·η^2-C≡C interactions. Such supramolecular aggregation process is preferred for orthomercurated molecules **22** with the least steric bulk. The absorption and emission properties of **22–29** are dominated by mildly mercury-perturbed organic π–π^* transitions, which are consistent with the results obtained from theoretical density functional theory (DFT) calculations. The emission maximum is bathochromically shifted for the *p*-nitrophenyl substituent relative to the 9-anthryl congener.

3.2. Compounds with fluorene groups

Much recent attention was paid to the employment of fluorene spacers in the formation of di-, oligo- and polymetallaynes [85]. The fluorene structural motif offers a rigidly planar biphenyl group in the backbone. The ease of structural modification and knowledge of the structure–property relationships of polyfluorene homopolymers and copolymers as well as their oligomers render tie fluorene-containing compounds very attractive candidates in the advance of new functional materials for optoelectronics and chemosensing applications [86]. By virtue of the high thermal and chemical stability and high emission quantum yields, fluorene-based derivatives are shown to be excellent materials for small-molecule and polymer light-emitting diodes (LEDs) [86–91]. In this connection, the following section will give a summary of the recent research efforts in our group devoted to the developments of fluorene-derived mercury alkynyls. A series of mono- and diethynyl fluorene-based precursors can be used as the synthons to produce thermally stable mono-, di-, oligo- and polynuclear complexes of mercury(II) according to the classical dehydrohalogenative coupling procedures. A family of dimercury(II) bis(alkynyl) complexes **30–36** constituted by various fluorenyl spacers were synthesized in good yield (Fig. 7) [92,93]. However, attempted derivatization of **35** to its dicyanomethylene-substituted species

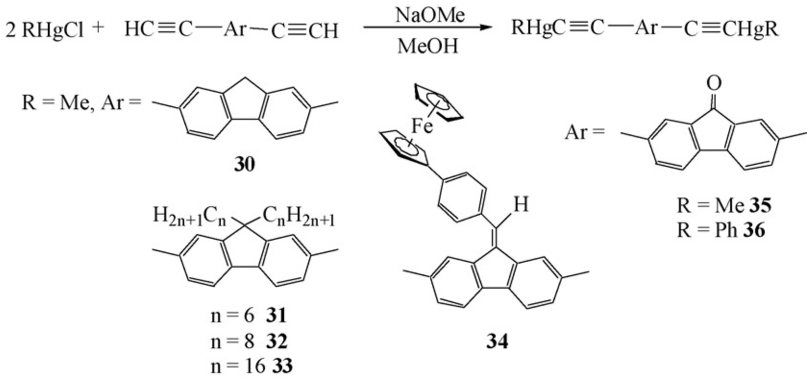

Fig. 7. Synthetic pathway to **30**–**36**.

has met with little success. The three-dimensional structures of **32** and **35** were confirmed by single-crystal X-ray diffraction studies (vide infra). By changing the substituents at C-9 position of fluorene ring, the optical bandgap (or onset of absorption), and the absorption and emission properties of these mercury-containing complexes can be chemically tuned, leading to diverse photophysical and redox properties. The energy gap generally follows the order **30** > **31** ≅ **32** ≅ **33** > **34** > **35** ≅ **36**. Because of the accessible low-lying π* orbitals of CO, the fluorenone-based complex gives a smaller energy gap. The similar spectral patterns for the mercury complex and its ligand precursor are suggestive of the ligand-dominating emissive state. As far as the central fluorene ring is concerned, the emission spectra of **30** and **35** having different fluorene moieties show very similar emission patterns with energy bands at 567 (for **30**) and 597 nm (for **35**) with a wavelength shift of 30 nm (Fig. 8(a)). The difference can be accounted for by the higher degree of π-conjugation of the fluorenone unit which increases the overlap with π*(C≡CR) to stabilize the low-lying π* orbital. Similarly, an order of emission energies of **36** > **35** is expected based on the different σ-donating capacity of the hydrocarbyl groups, viz., Me > Ph. The results for these mercurial compounds were systematically correlated to those for the closest neighbors of group 10 platinum(II) and group 11 gold(I) elements in the periodic table [92–94].

While there is a world-wide interest in conjugated polymer electroluminescence for the perceived potential in the low-cost fabrication of large-area LEDs through simple processing methods, the utilization and characterization of triplet excitations in phosphorescent polymer devices is particularly important nowadays for the enhancement of their device efficiencies [6]. The ultimate efficiency of LEDs is controlled by the fraction of triplet states generated or harvested [95–99]. In this regard, polymetallayne systems have been widely studied as model systems to explain aspects of the photophysics of electronically excited states in such conjugated polymers in which the heavy metals increase the spin-orbit coupling, rendering the spin-forbidden phosphorescence (triplet emission) partially allowed. Thus, in contrast to hydrocarbon conjugated polymers, the triplet excited state is experimentally accessible by using optical methods. It would be useful to know how the triplet emission efficiency can change with the chemical structure so that the relative separation of the energy bands can be manipulated and hence, the energy of the triplet excited state can be harvested directly. In accordance with the energy gap law, the intersystem crossing (ISC) rate depends exponentially on the energy gap to the nearest triplet excited state [100,101]. Therefore, the relative positions of singlet and triplet excited states strongly govern the ISC rate into the triplet manifold. In the past two decades, the photoluminescent behavior of oligomeric and polymeric acetylides of

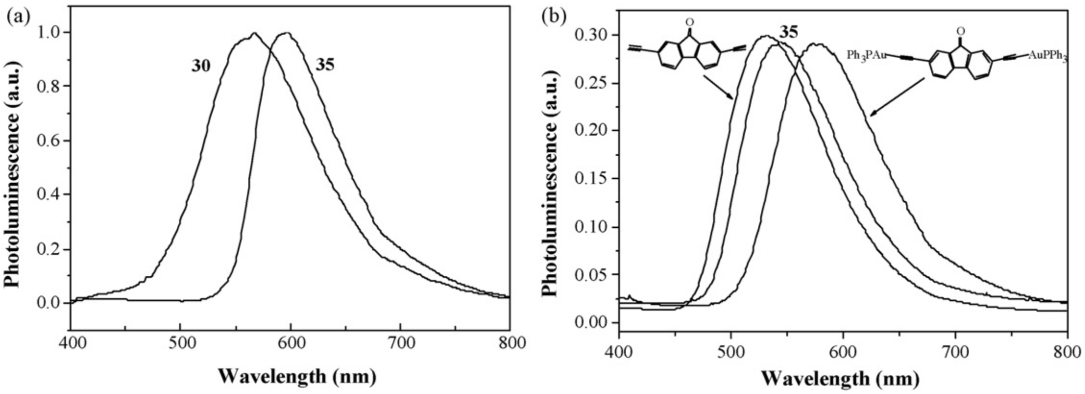

Fig. 8. (a) Effect of fluorene spacer and (b) effect of metal groups on the PL spectra in CH_2Cl_2 at 298 K [92].

platinum(II) and gold(I) complexes has aroused much research attention where spin-forbidden phosphorescence can be identified clearly [21]. To our knowledge, there was no literature precedent of studying the photophysics and structural properties of soluble mercury-based polyynes of this type. We contend that group 12 heavy mercury atom, with its propensity to enhance spin-orbit coupling, should be equally suitable for harvesting the energy of triplet excitons. While linear polymeric copper and mercury acetylides of the form $[–MC{\equiv}C(p\text{-}C_6H_4)C{\equiv}C–]_n$ were reported over 45 years ago [41] and metal-alkynyls of group 12 elements have been known for many years, the designed synthesis, chemistry and photophysics of mercury-alkynyl compounds, however, has not been so thoroughly studied. Low solubility and poor tractability of compounds is a major difficulty associated with the preparation of conjugated mercury(II) σ-acetylide polymers, which generally hampered their purification and spectroscopic characterization. We have reported for the first time a novel series of soluble well-defined high-molecular-weight d^{10} mercury(II) polyyne polymers with 9,9-dialkylfluorene spacers **38**–**40**, which could render $^3(\pi\pi^*)$ phosphorescence through efficient ISC by ligation to the Hg(II) center [102]. However, starting from 2,7-diethynylfluorene, only an intractable off-white solid **37** was obtained, indicating that long-alkyl chains should be introduced as solubilizing groups to produce these soluble organometallic mercury(II) polyynes. The synthesis of **37**–**40** involves room-temperature base-initiated mercuration reaction of 9,9-dialkyl-2,7-diethynylfluorenes with $HgCl_2$. They exhibit very good solution-processability in solvents such as CH_2Cl_2 and $CHCl_3$. The degree of polymerization is very high in these polyynes as revealed from GPC and NMR end group analysis. The high structural regularity of the polymers was confirmed by NMR studies. In attempts to model the polymers and gain added insight, complexes **30**–**33** were also prepared, in which one coordination site on Hg(II) is capped by a Me group [92,102]. Complex **32** showed a single ^{199}Hg NMR signal at $\delta = -453$ (versus $\delta = -847$ for MeHgCl against Me_2Hg standard), indicating polarization of the Hg–C≡ bonds. The X-ray crystal structure of **32** also helped to establish polymer structure in the solid state and to correlate the photophysical properties with the structural data. The formation of solid-state aggregates in thin films for the polymers is shown by the growth of a new absorption band at around 365 nm as a nonsolvent such as MeOH is continuously being added to the polymer solution in $CHCl_3$, which corresponds to the strongest absorption peak observed in the solid state (Fig. 9) [103]. The long-side chains in **38**–**40** should suppress aggregation or at least delay its onset, and changes in absorptions were observed for **39** only after addition of approximately 80% MeOH. This is also supported by the structural data in which mercurophilicity was shown to exist (vide infra). Polymers **38**–**40** are thermally stable and they exhibit decreasing decomposition temperatures with the chain length of R groups. Each polymer shows two stepwise losses in the TGA curve, corresponding to the elimination of two alkyl groups from their molecules. For **39**, **41** and **42** were also prepared as the oligomeric model complexes for the electronic properties of the corresponding polyyne [104].

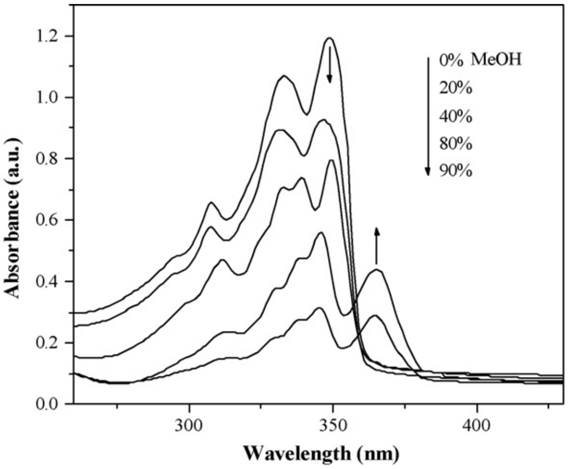

Fig. 9. Aggregation phenomenon in the absorption spectra of **39** at different volumes of MeOH at 298 K [102].

Polymers **38**–**40** all show similar structured absorption bands in the near UV region, which are associated with the organic $^1(\pi\pi^*)$ transitions, possibly with some admixture of metal orbitals (Fig. 10). The absorption energies are virtually insensitive to the length of C-9 alkyl substituent on the fluorene ring for **38**–**40**. The transition energies of the polymers are lowered with respect to those of **31**–**33**, suggesting a well-extended singlet excited state in the polymers. The PL spectra display a red-shift on going from binuclear to polynuclear structures. In dilute fluid solutions, there is a singlet emission peak near 400 nm for **38**–**40** (Fig. 10). Comparing with the solution PL data, the thin film singlet emissions in **38**–**40** appear broad at 290 K and are red-shifted, probably as a result of interchain interactions due to aggregate formation. Phosphorescence from these organometallic materials is generally restricted to low-temperature glasses, but the heavy-atom effect exerted by Hg(II) results in enhanced spin-orbit coupling and consequently the occurrence of long-lived triplet emission. At 11 K, phosphorescence emissions emerge around 570–590 nm for **38**–**40** with the long-emission lifetimes of 28–42 μs. The integrated intensity

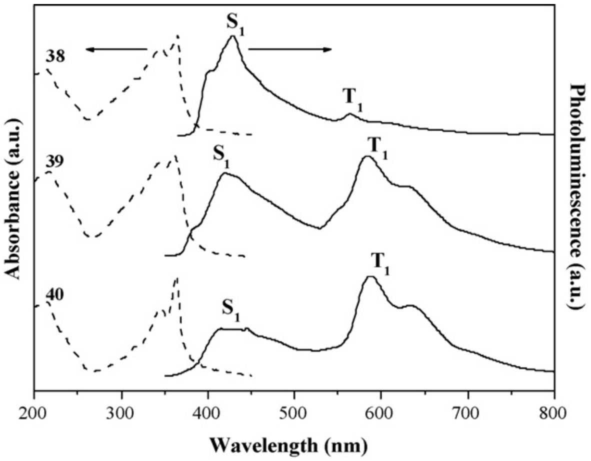

Fig. 10. Absorption (298 K) and PL(11 K) spectra of thin films of **38**–**40** [102].

of the phosphorescence relative to fluorescence was shown to increase as the value of m increases from **38** to **40**. We note that the order of ISC efficiency is **40** > **39** > **38**. The ISC rate is also higher in the polymers than in the dinuclear complexes. Values of energy gap between S_0 and T_1 levels were found to be 2.10–2.23 eV for **38**–**40**, which can be compared to those observed in some PPEs (1.90 eV) [105] and [Cy_3PAu]-capped PPEs (1.98–2.04 eV) [26]. The S_1–T_1 gaps for **38**–**40** lie within the range of 0.73–0.79 eV which match well the corresponding gaps of 0.7 ± 0.1 eV for similar π-conjugated Pt(II) and Au(I) polyynes, and are close to the gaps estimated for a series of relevant organic-based polymers [106,107].

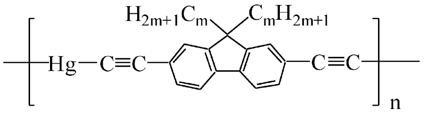

m = 0 **37**
m = 6 **38**
m = 8 **39**
m = 16 **40**

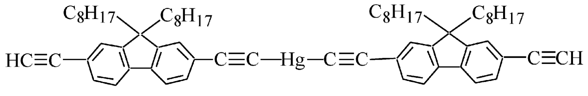

41

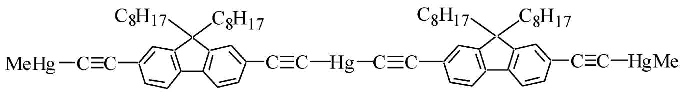

42

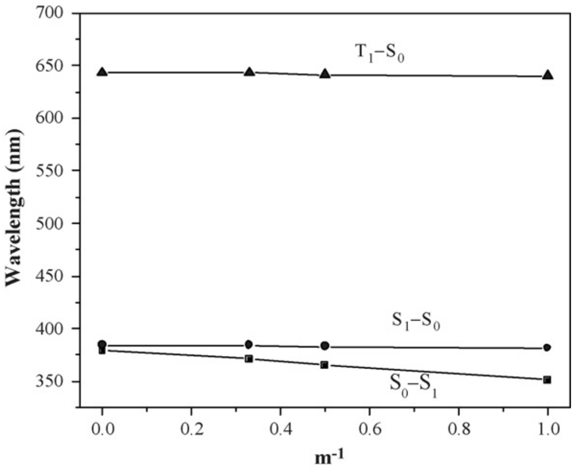

Fig. 11. Dependence of absorption and PL data on m^{-1} based on theoretical data.

Our pioneering report on **38**–**40** and their diynes **31**–**33** have led to detailed theoretical investigation by Feng et al. on these molecules and their purely organic counterparts using the Hartree–Fock and DFT calculations on these d^{10} mercury polyynes in order to establish their structure–property relationship [108]. The computational results show that there is a weak electronic interaction between the metal-based fragment and the π-conjugated organic groups, and thus the photophysical properties are mainly based on the diethynylfluorene π-conjugated segment with little contribution from the metal center. The role of the metal center can be described as weak delocalization coupled with strong localization characteristics along the organometallic polymer chain. Molecular orbital calculations found that the energy gap decreases from 3.85 eV (**30**) to 3.64 eV (**43**) and 3.56 eV (**44**) for the mercury oligoynes but the value decreases at a higher rate in the metal-free oligo(fluorenyleneethynylene)s **I**–**III**, which is in line with the larger conjugation and π-electron delocalization along the organic chain and relatively weaker conjugation along the corresponding Hg polyyne chain. The lowest singlet and triplet excited states have been studied by the singles configuration interaction (CIS) method and time-dependent density functional theory (TDDFT). Both singlet and triplet excited states of the polymer are localized mainly on the conjugated ligand segment. Through the chain length dependence of emission energies, a singlet emissive peak at 384.9 nm was obtained for the polymer by extrapolation, which is comparable to 382 nm observed experimentally from the solution phase PL spectrum. Based on the DFT results, the relationships between calculated absorption, fluorescence and phosphorescence wavelengths as a function of reciprocal chain length were derived and shown in Fig. 11.

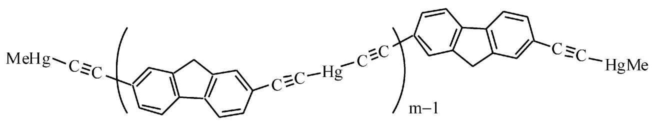

m = 1 **30**
m = 2 **43**
m = 3 **44**

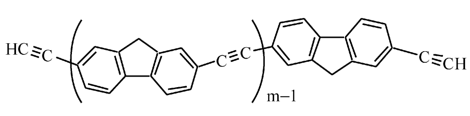

m = 1 **I**
m = 2 **II**
m = 3 **III**

We recently reported a useful procedure to transform dissolved inorganic mercury(II) into stable mercury(II) acetylide derivatives functionalized with a range of monosubstituted fluorene units which show interesting photophysical properties suitable for various material and analytical applications [109]. Luminescent mononuclear mercury(II) mono- and dialkynylated complexes containing substituted fluorene and fluorenone units **45**–**56** were prepared in good yield by mercuration of terminal acetylenes R–C≡CH with MeHgCl and $HgCl_2$ at room temperature. The structures of these organomercurial compounds were characterized by IR and NMR spectroscopies, elemental analysis and FAB mass spectrometry. Their optical and photoluminescence spectra were also studied. The structural features of **45** were elucidated by X-ray crystallography in which there is an indication of weak mercurophicity among the molecules in the solid state.

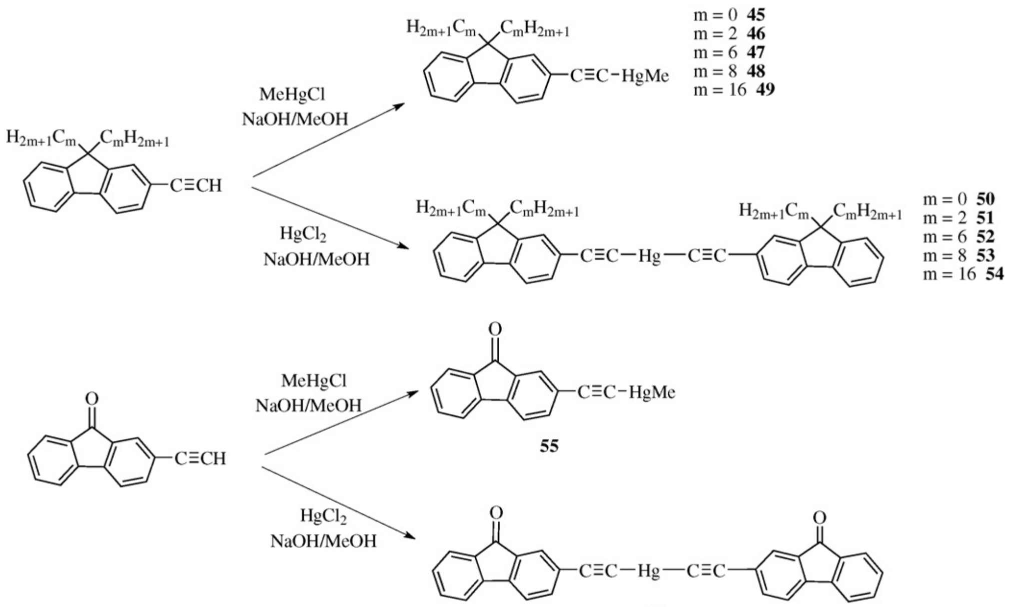

55

56

Recently, the energy gap law has been established for triplet states in metal-containing conjugated polymers and their model complexes whereby the non-radiative phosphorescence decay rate increases exponentially with decreasing energy gap to the nearest triplet excited state. It would be a critical issue to rationalize the factors for controlling the spatial extent of the singlet and triplet energy levels in governing the singlet–triplet gap. While detailed studies on the synthesis and optical properties are now known for **31** and **38**, compounds **57** and **58** incorporating 9,9-dihexylfluorene and butadiynyl units were prepared in order to determine the spatial extent of the lowest singlet and triplet excited states with the acetylenic chain length [110]. The polymer **58** was isolated as a soluble high-molecular-weight copolymer. While these carbon-rich metallaynes constitute an intriguing class of optoelectronically tunable compounds, they provide good opportunities in tailoring molecule-based functional properties. The energy of the S_1 excited state decreases on going from **38** to **58**.

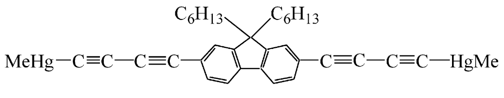

57

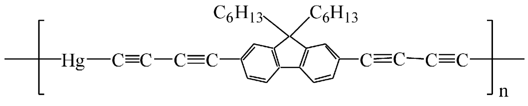

58

We also reported a high-yield synthetic route to the mercury polyyne **59** based on 9,9-bis(4-ethynylphenyl)fluorene [111]. Polyyne **59** appears to be more thermally stable than **38–40**. Reduced conjugation in the presence of the non-π-conjugated segment shifts the optical bandgap for **59** to the blue when compared with **10**. However, only the lower-molecular-weight oligomeric fraction of **59** can dissolve in CH_2Cl_2 and $CHCl_3$. Dimercury(II) complex **60**, as a model of **59**, was also prepared. Systematic investigations of the PL properties for **59** and **60** and its Pt(II) and isoelectronic Au(I) congeners were made. The extent of π-conjugation of the compounds follows the experimental order Hg > Au > Pt. Mercury ion can induce heavy-atom effects in the enhancement of ISC rate and the harvesting of organic triplet emission (Fig. 12), but the effect is less significant for Hg(II) than Pt(II). Such work is significant in that the deliberate use of tetrahedral conjugation-breaking sp^3-hybridized carbon atom of the diphenylfluorene unit can limit the effective conjugation length and gives rise to more efficient phosphorescence emission in metal-containing aryleneethynylenes (Fig. 13).

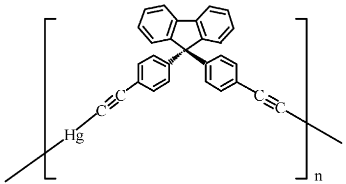

59

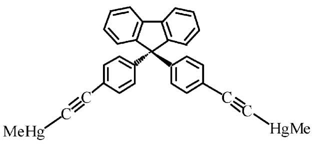

60

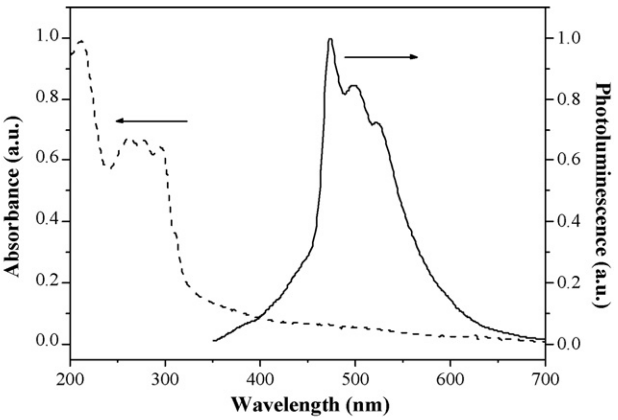

Fig. 12. Absorption (293 K) and PL (11 K) spectra of **59** as thin films [111].

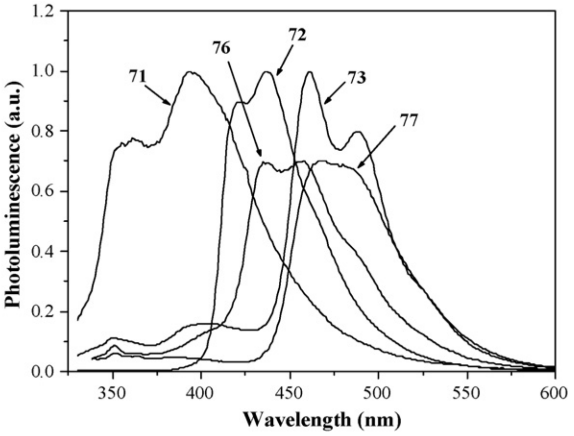

Fig. 13. PL spectra of some dimercury diacetylide complexes containing oligothiophene and bithiazole spacers in CH_2Cl_2 at 298 K [115].

3.3. Compounds with carbazole groups

Among the heterocyclic derivatives, the carbazole ring has emerged as an excellent building block in the synthesis of a variety of optoelectronic materials [85]. While recent advances based on the exploitation of carbazole as the chromophore for the synthesis of branched molecules, oligomers, polymers or dendrimers have spurred considerable interest, they are, however, largely confined to organic systems. Carbazole-based coordination/organometallic compounds have been much less explored. In particular, the chemistry of metallopolymers derived from derivatized diethynylcarbazole moieties represents a topical area that is still in its infancy and very few reports are known in the sensitization of phosphorescence of carbazole using heavy-metal effects. By virtue of the excellent functional properties of carbazole derivatives for organic materials [8], we feel it highly appropriate to incorporate 9-aryl-substituted carbazole unit via 3,6-positions into the metallopolyyne system so that some novel transition metal-based polymeric and oligomeric assemblies with an emissive state possessing rich triplet content and high-energy triplet state can be developed. A new series of mercury diynes **61–65** containing various *p*-substituted 9-phenylcarbazole moieties have been prepared and optically characterized [112,113]. However, their corresponding polyynes are essentially intractable materials for satisfactory photophysical characterization. The molecular structures of **62** and **63** were established by X-ray structural analyses. The heavy-atom perturbation of Hg(II) ion in triplet-light-harvesting and the influence of the 9-aryl moiety of carbazole on the phosphorescent properties of these organomercurial acetylide materials were examined and compared to those for their Pt(II) and Au(I) counterparts. The absorption data were found to be relatively insensitive to the nature of the aryl substituent X on the carbazole ring, in line with the notion that the carbazolyl unit tends to hinder π-conjugation along the main chain. It is obvious that the emission wavelength does not seem to vary much with the type of X group in each series. For each metal class, a strong phosphorescence band was observed at low temperature and there is a small but notable shift in the wavelength to the blue along the sequence Pt → Au → Hg, in line with the absorption trend. We note that the $N(C_6H_4X)$ group of carbazole can reduce conjugation relative to the bi(phenylene)-linked compounds, leading to a marked blue-shift in the absorption maxima. The present work indicates that the efficiency of organic triplet emissions harnessed through the heavy-atom effect of these metals in the main chain generally follows the order Pt > Au > Hg. All of these carbazole-containing materials with high-energy T_1 states of 2.68 eV or higher show high phosphorescence efficiencies at low temperatures. The work has also been developed to the alkylated substituent such as butylcarbazole in the formation of **66** and **67** [114]. Mercury polyyne **67** is not completely soluble in organic solvents and GPC measurements suggest a low molecular weight distribution with $M_W = 4630$ and $M_n = 4690$.

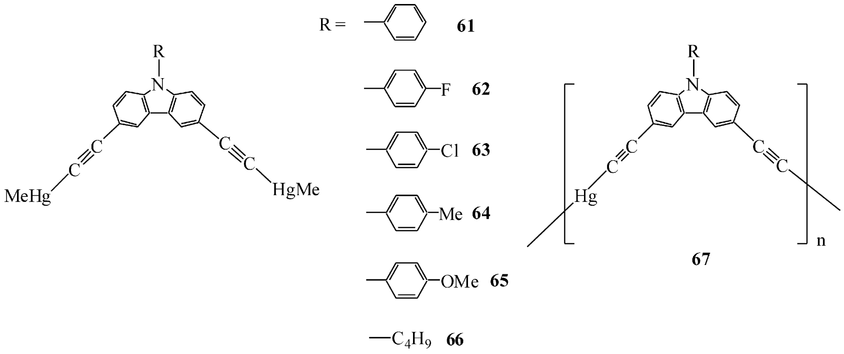

3.4. Compounds with oligothiophene and related groups

Among the vast majority of organic backbones used, conjugated thiophene derivatives have been extensively explored due to their chemical stability, synthetic accessibility and their growing importance in the rapidly expanding field of electronic and optoelectronic devices and as the fluorescent biomarkers in biological research [20]. A new series of luminescent dimercury(II) diacetylide complexes of oligothiophenes **68–73** and bithiazoles **74–77** are prepared [115]. Their electronic, photophysical and structural properties were studied and correlated to the chain length and electronic nature of the central five-membered heterocyclic conjugated systems. With increasing thiophene content, the absorption and emission features are both red-shifted and the emission quantum yields are increased. In the presence of electron-withdrawing imine nitrogen atoms, the optical spectra for the bithiazole derivatives also show a significant bathochromic shift when compared to their bithienyl counterparts. The insoluble polymers **78–80** were shown to display very similar IR stretching frequencies as for the dimercury(II) model compounds **68–73** and the crystal structures of **68** and **69** have been established to study the metal–metal and ligand–ligand interactions in such mercury polyyne systems. These structures were highlighted by the extensive mercuriophilicity observed among Hg atoms. The dependence of photophysical data with the oligothienyl chain length was examined. The results were also correlated to the theoretical data obtained by DFT calculations. The metal contributions based on the Mulliken population analysis to the HOMO and LUMO are small (HOMO 3.0, LUMO 20.0% from each Hg for **68**; HOMO 1.5, LUMO 7.0% from each Hg for **69**). Increasing conjugation through more thienyl rings leads to a decreased transition energy and an increase in the molar absorption coefficients for **68–70** as well as **71–73**. Thus, a red shift of 75 nm is observed from **68** to **70**, whereas the shift is 71 nm from **71** to **73**. However, the value of the red-shift induced by the end substitution of Hg(II) groups decreases with increasing number of thienyl units (m). These results are also consistent with the mercury-based orbitals contributing less to the HOMO and LUMO levels as m increases and hence π-conjugation increases. The orders of emission energies **68** > **69** > **70** and **71** > **72** > **73** are expected in moving from the monothiophene to the terthiophene. With increasing thiophene content, the absorption and emission features are both red-shifted and the PL quantum yields are increased.

Moreover, a high-yield synthesis to some luminescent binuclear mercury(II) bis(alkynyl) complexes bearing bithiazole conjugated units was presented. A thiazole unit can be regarded as a hybrid of the thiophene and pyridine groups that can be a valuable spacer for controlling the bandgaps of these metallated materials. In the presence of electron-withdrawing imine nitrogen atoms, the optical spectra for the bithiazole derivatives also show a significant bathochromic shift when compared with their bithienyl counterparts. Quantum yield values associated with 4,4′-di(*t*-butyl)-2,2′-bithiazole-linked complexes are higher than those for the bithienyl congeners. The absorption peak of **75** (or **77**) is also red-shifted relative to **74** (or **76**), presumably due to the more extensive conjugation via the π-phenylene unit along the π-donating capacity of the OMe moiety in the former case. Recent exploitation of some luminescent derivatives of inorganic mercury and methylmercury bearing 4,4′-di(*tert*-butyl)-5-ethynyl-2,2′-bithiazole ligand **81** and **82** in the development of a simple procedure for the speciation of mercury(II) by HPLC analysis with UV detection was described [116]. Such an analytical protocol offers a new approach for the simultaneous determination of inorganic Hg(II) and MeHg(II) in aqueous solutions, which will be beneficial to analytical green chemistry in the long run (vide infra).

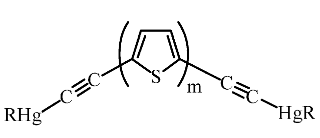

R = Me, m = 1 **68**
R = Me, m = 2 **69**
R = Me, m = 3 **70**
R = Ph, m = 1 **71**
R = Ph, m = 2 **72**
R = Ph, m = 3 **73**

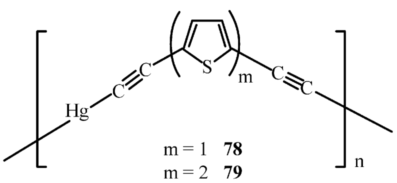

m = 1 **78**
m = 2 **79**
m = 3 **80**

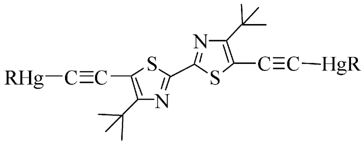

R = Me **74**
R = Ph **76**

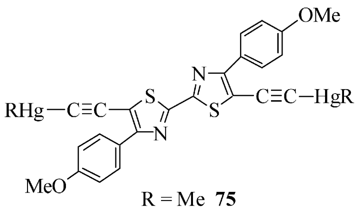

R = Me **75**
R = Ph **77**

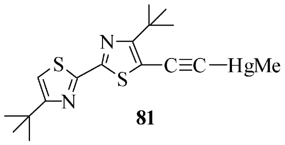

81

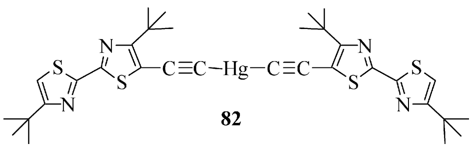

82

3.5. Heterometallic compounds

A black ethynyl derivative of a mixed tungsten–mercury tetrathiometallate complex **83** was prepared from its yellow ethenyl complex following a topochemical conversion via spontaneous dehydrogenation of the vinyl group. The crystal structure of **83** was determined which contains half a solvate molecule of acetaldehyde [117]. 2-Ethynyl-7-(2-ferrocenylethynyl)fluoren-9-one serves as a versatile ferrocenylacetylene complex and can be used to give an iron–mercury heterometallic complex **84** [118]. Crystal structure analysis reveals that there are no apparent weak intermolecular Hg···Hg interactions or π-stacking of the aromatic rings in **84**. The closest intermolecular contacts in **84** are attributed to the Hg(1)$\cdots$O(1) (3.314 Å) and Hg(1)$\cdots$H(6A) (3.224 Å) interactions. The redox chemistry of these mixed-metal species has been investigated by cyclic voltammetry and oxidation of the ferrocenyl moiety is facilitated by the presence of HgMe unit and increased conjugation in the chain through the ethynyl and fluorenone linkage units.

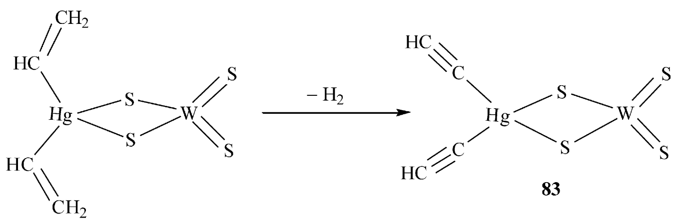

83

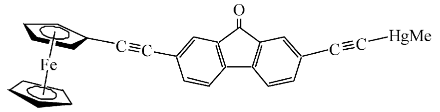

84

A catalytic cycle for the demercuration of $Hg(C{\equiv}CR)_2$ (R = Ph, Tol, ^{n}Bu) in the presence of $[RhCl(CO)(PPh_3)_2]$ to afford buta-l,3-diynes RC≡CC≡CR was proposed in which the 18-electron intermediate **85** was isolated [119]. In a related connection, an analogous complex **86** was formed by reaction of $[Ir(SeC{\equiv}CR)(CO)(PPh_3)_2]$ with $Hg(C{\equiv}CTol)_2$ This can be compared to the Collman's synthesis of $[Ir(C{\equiv}CPh)Cl(HgC{\equiv}CR)(CO)(PPh_3)_2]$ from Vaska's complex and $Hg(C{\equiv}CPh)_2$ [120].

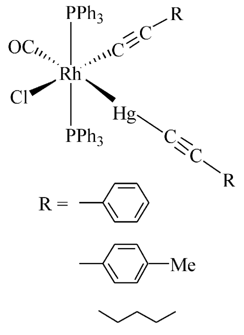

85

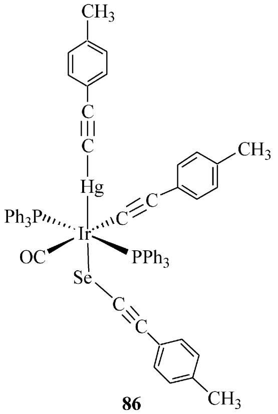

86

The use of $Hg(C{\equiv}CR)_2$ (R = Ph, Tol, CMe_3) as new organometallic templates in the formation of interesting metal-organic polymeric assemblies **87–89** and their molecular models **90–92** have been described by Mingos and co-workers [121,122]. Some coinage metals such as Cu(I) and Ag(I) ions were demonstrated to coordinate to the alkynyl units via π-bonding interactions. Crystal structures of **88** and **91** (M = Ag, X = BF_4) were obtained in which weak anion$\cdots$cation interactions were observed. The structure of **88** consists of a polymeric skeleton with the resulting helices cross-linked by C–H$\cdots$π contacts. The presence of various supramolecular interactions was apparent in the X-ray structures of these multimetallic aggregate molecules.

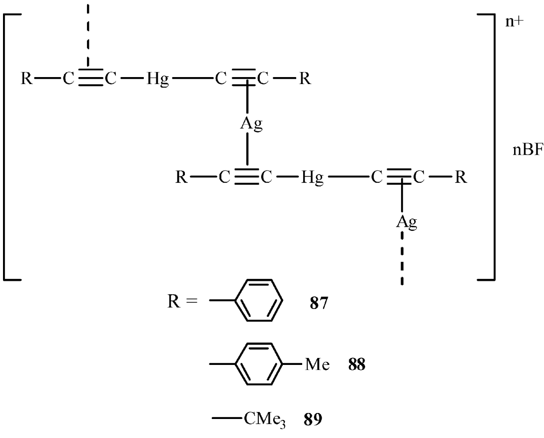

87 **88** **89**

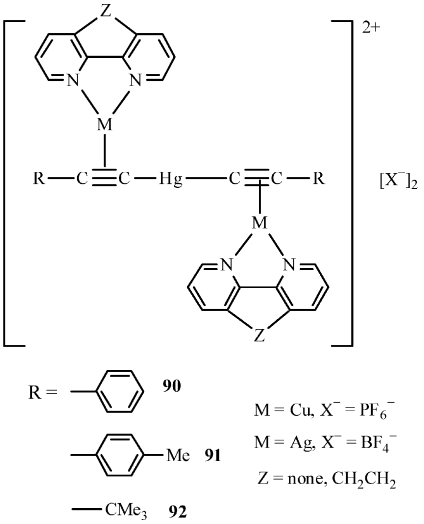

90 **91** **92**

M = Cu, X⁻ = PF_6^-
M = Ag, X⁻ = BF_4^-
Z = none, CH_2CH_2

η^2-Coordination of the alkynyl ligands to mercury is also commonplace in organometallic chemistry. Bimetallic Pt–Hg complexes **93** and trinuclear Hg–Pt–Hg alkynyl complexes **94** were made by reactions of the appropriate Pt-alkynyl precursors with HgX_2 in a 1:1 and 1:2 stoichiometry. The structure for **93** (X = Br, R = $SiMe_3$) was established by X-ray diffraction method in which the measured platinum–mercury distance is about 3.627 Å [123]. Similar methodology has recently been applied to the lighter cadmium system and the report provides an access to some mixed-metal alkynyl platinum–cadmium complexes which can display interesting luminescence properties [124]. Likewise, the heterotrimetallic double-tweezer compound **95** was formed by complexation of two $HgCl_2$ units onto the corresponding planar tetraethynylplatinum complex and its crystal structure was reported in which the geometry at mercury is distorted tetrahedral. There is no evidence of significant interaction between Pt and Hg atoms in **95** [125]. Complexation of some mercury salts with organometallic *cis*–bis(alkynyl) tweezer complexes of titanium(IV) and platinum(II) readily produced various heterobimetallic titanium–mercury **96** and **97** and platinum–mercury π-tweezer species **98** [126]. All the compounds were characterized by elemental analysis and conventional spectroscopic (IR, NMR and MS) techniques.

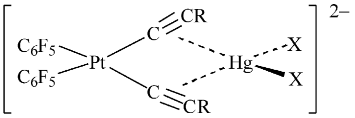

X = Cl, R = Bu or SiMe$_3$
X = Br, R = Bu or SiMe$_3$
X = I, R = Bu or SiMe$_3$

93

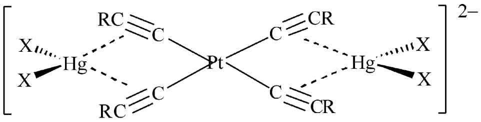

X = Cl, R = Bu or SiMe$_3$
X = Br, R = Bu or SiMe$_3$
X = I, R = Bu or SiMe$_3$

94

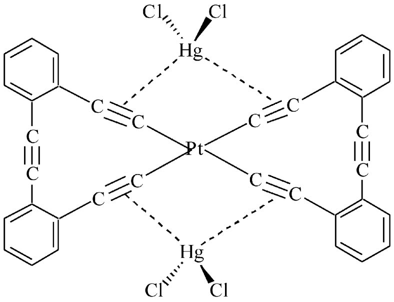

95

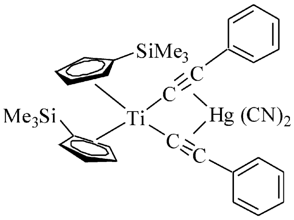

96

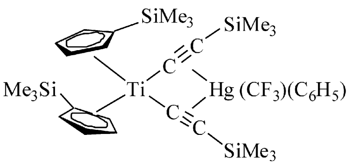

97

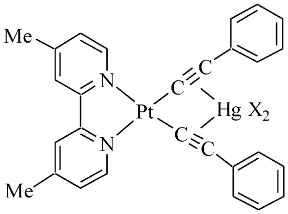

X = Br or I

98

There are numerous examples of mercury(II) complexes containing oligoynyl units along the molecular chain. Fischer et al. have reported the synthesis of trinuclear biscarbene complexes **99** and **100** along with the X-ray structure of the latter complex [127]. They also extended the work to the higher oligoynyl homologue **101** and **102** by mercuration of the hexatriynylcarbene complex $[(CO)_5W{=}C(NMe_2)C{\equiv}CC{\equiv}CC{\equiv}CH]$ with $HgCl_2$ in the presence of ^{n}BuLi [128]. Complexes **101** and **102** contain two 2,4,6-heptatriynylidene fragments linked directly to Hg(II) ion in a linear fashion. Bruce and co-workers have prepared two mixed metal bis(butadiynyl) complexes of gold and mercury **103** and **104** by direct reaction of $Hg(OAc)_2$ with diynylgold(I) phosphine complexes $Au(C{\equiv}CC{\equiv}H)(L)$ ($L = PPh_3$, $P(Tol)_3$) and their IR, ^{1}H and ^{31}P NMR data were reported [129]. The same research group further explored the synthesis and structural characterization of some rod-like diruthenium tetrayne complexes **105** and **106** bridged by a central Hg unit to afford the Ru–C_4–Hg–C_4–Ru chain [130]. The electronic structures of these molecules were investigated using molecular orbital calculations with the aid of EH and DFT methods. The novel bis(tricarbido) mercury complexes **107** and **108** were prepared from the fluoride-mediated desilylation of the propargylidyne complex $[[W{\equiv}CC{\equiv}CSiMe_3](CO)_2\{HB(pz)_3\}]$ (pz = pyrazol-1-yl) in the presence of $HgCl_2$. The structure of **108** was confirmed by X-ray crystallography as a dmso hexasolvate and its spectroscopic and absorption data were reported. The catalytic demercuration of both **107** and **108** to yield dimetallaoctatetraynes was also studied [131].

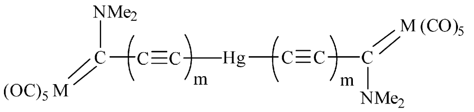

M = Cr, m = 1 **99**
M = Mo, m = 1 **100**
M = Cr, m = 3 **101**
M = Mo, m = 3 **102**

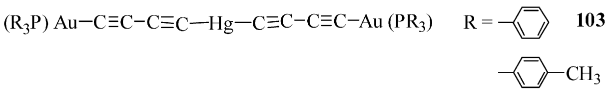

103

104

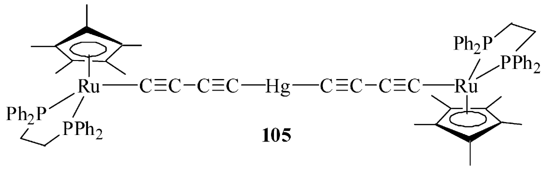

105

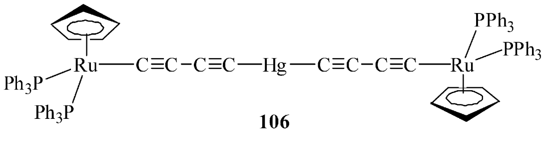

106

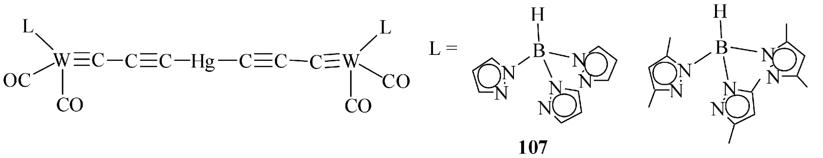

107

108

The first example of a rigid-rod heteronuclear platinum-mercury polyyne polymer **109** and its model compound **110** was reported and the polymer is remarkable in its good solubility in organic solvents and highly transparent nature in the visible regime [104]. It displays excellent optical power limiting (OPL) at a high linear transmittance (*T*) of 92%, which outperforms that of current state-of-the-art materials such as C_{60}, metalloporphyrins and metallophthalocyanines. The model complex **110** was studied for comparison of the electronic and structural properties with **109** and the effect of chain length in the OPL phenomenon. It is clear from such work that mercury plays a crucial role in the enhanced OPL performance. The results were supported both experimentally and theoretically. Coupling of Hg(II) to the main chain of **41** breaks the π-conjugation to a certain extent but favorably optimizes the transparency/nonlinearity trade-off. It manifests a very low OPL threshold of 0.083 J/cm^2 at $T = 92\%$. Such an approach can be exploited for the realization of how to increase the optical transparency range while maintaining the OPL responses of the polymers constant.

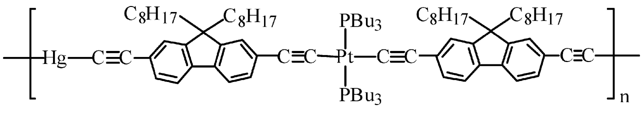

109

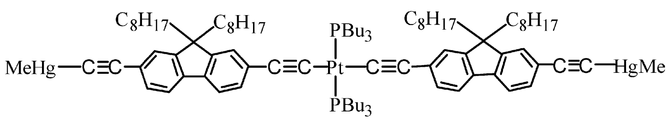

110

4. Structural features and mercurophilicity

It is now widely recognized that Au(I) complexes often form solid-state structures which involve attractive secondary interactions, i.e. the aurophilic effect. The role of aurophilicity in the solid-state packing was comprehensively discussed [23–25,34,35]. The Au· · ·Au distances are typically 3.0–3.6 Å, longer than the Au–Au distance in gold metal but shorter than the sum of the van der Waals (VDW) radii. Theoretical analysis has attributed this to electron correlation enhanced by relativistic effects. For other d^{10} ions, there are fewer examples of similar interactions. It has been suggested that, akin to the metallophilic interactions displayed by Au(I), Ag(I) [132,133] and Cu(I) [134], complexes based on Hg(II) should display analogous mercurophilicity. For Hg^{2+}, evidence for intermetallic bonding interactions is not strong [135]. While bis(alkynyl)mercurials are known to crystallize with mercurophilic interactions that bring adjacent alkynyl groups within close proximity, relatively few complexes displaying short Hg(II)· · ·Hg(II) separations have been reported to date. The discussion on whether or not these short distances have to be considered as clear indications of metallophilic interactions in mercurial compounds is still open to much debate. The VDW radius of mercury of up to 2.2 Å has been proposed recently [136,137], which is conceived to be a better estimate than the value quoted by Bondi in 1964 [138]. Intermolecular Hg· · ·Hg interactions can be found in a number of non-alkynyl organomercury compounds such as $[MeHg(SC_4H_2N_2Me)]$ (3.10 Å) [139], $Hg(SiMe_3)_2$ (3.1463 Å) [140], $(HgH_2)_n$ ($n = 2, 3$) clusters (4.077 and 4.449 Å) [141] and a mixed Hg_2Cu metallamacrocycle (3.203 Å) [142]. This distance is clearly shorter than twice the VDW radius of mercury (∼4 Å) and would seem appropriately classified as a manifestation of mercurophilicity. Indeed, alkynylmercurials have been less explored structurally according to the records by Cambridge Crystallographic Data Center (CCDC). Fig. 14 summarizes a list of recently established X-ray crystal structures for mono- and dinuclear mercury alkynyls in our group in the past 5 years. Table 1 gathers structural data around Hg center for published alkynyl complexes of mercury.

Mercury(II) alkynyl complexes possess a strong driving force for aggregation in the solid state, largely through mercurophilic attractions, possibly combined with other non-covalent contacts such as Hg· · ·C≡C interactions. Among these, over 50% of our reported structures exhibit various degrees of mercurophilic-

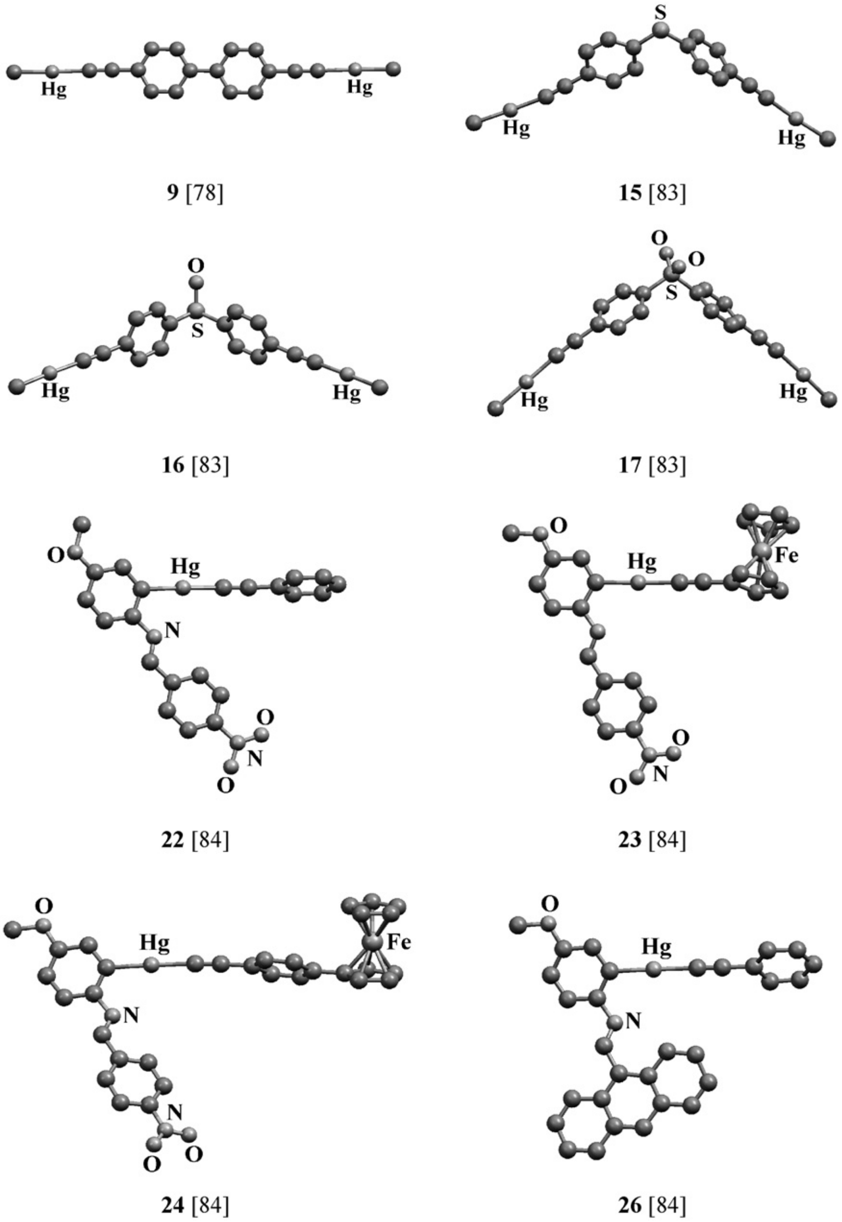

9 [78]

15 [83]

16 [83]

17 [83]

22 [84]

23 [84]

24 [84]

26 [84]

Fig. 14. X-ray crystal structures of mercury alkynyl complexes. Hydrogen atoms and all carbon atom labels are omitted for clarity.

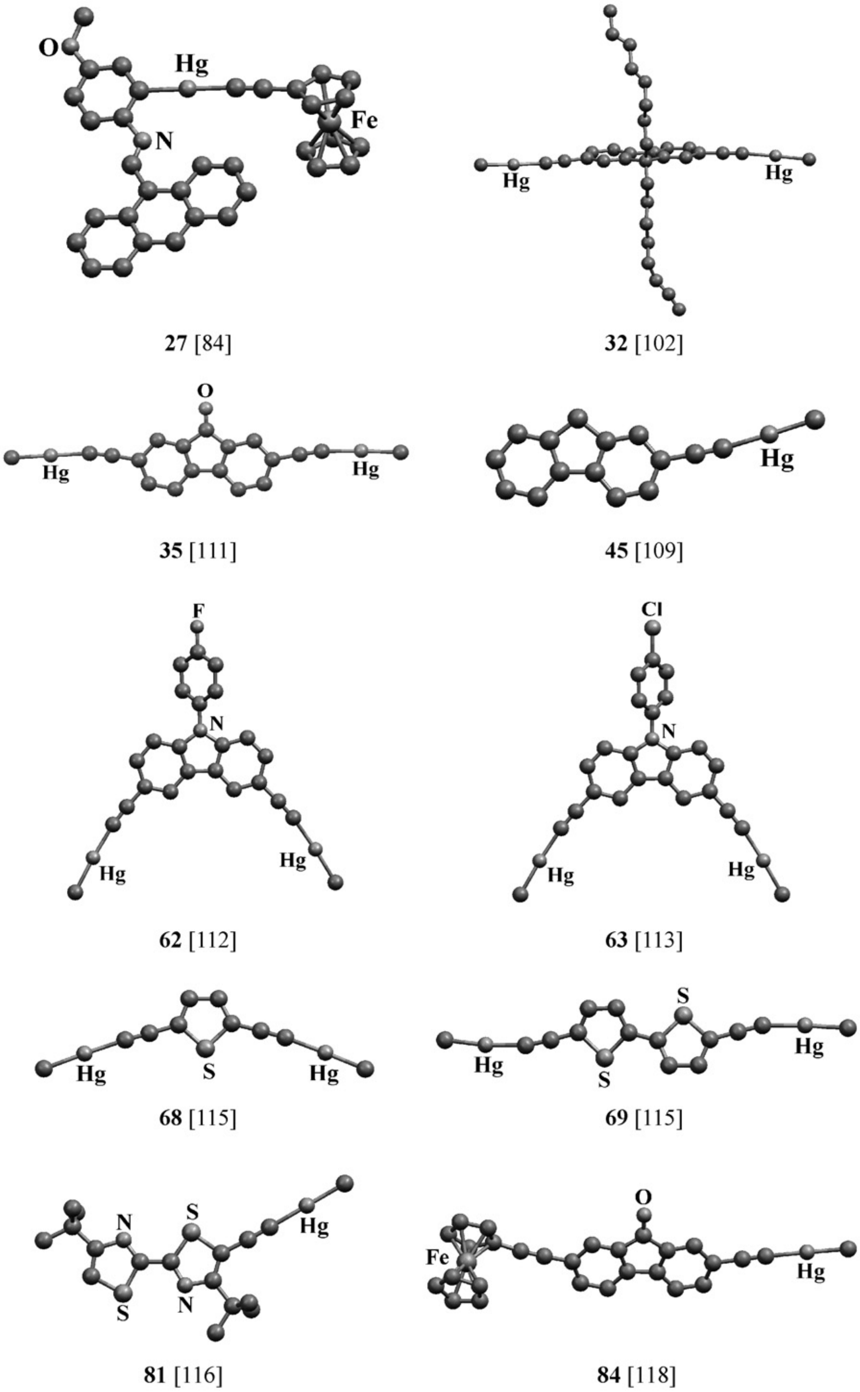

27 [84] **32** [102]

35 [111] **45** [109]

62 [112] **63** [113]

68 [115] **69** [115]

81 [116] **84** [118]

Fig. 14. (*Continued*).

ity (Fig. 15). The observed Hg···Hg separations are towards the upper limit of those accepted as representing metallophilic interactions. While the Hg···Hg contacts in each of these compounds indicate that each of the individual interactions is relatively weak, it is the large number of them that will play a supramolecular role and generate a significant driving force for solid-state aggregation in most cases. We believe that such mercurophilic forces are more than just van der Waals interactions in these chemical systems. For instance, there is a strong tendency for the molecules in **9** to aggregate together and the whole lattice structure is fully supported and stabilized by extensive non-covalent d^{10}–d^{10} Hg···Hg interactive vectors (ca. 3.833, 4.222 and 4.506 Å) that link up the individual molecules in an organized 3D polymeric network. The lattice is characterized by infinite linear chains of Hg atoms between adjacent molecules. Aggregation of each stack of these molecules also persists throughout the entire crystal lattice in a 3D space via weak Hg···Hg attractive interactions (3.833, 4.222 Å) to form another zigzag chains of Hg centers with the Hg–Hg–Hg angles of 67.8° and 60.2°. For **22**,

Table 1
Structural data for published mercury(II) alkynyl complexes

Complex	Hg···Hg (Å)	Hg–CH$_3$ (Å)	Hg–C≡ (Å)	C≡C (Å)	Hg–C≡C(η^2) (Å)	C–Hg–C (°)	Hg–C≡C (°)	References
$Me_3Si–C{\equiv}C–Hg–C{\equiv}C–SiMe_3$	3.76–4.07		2.00	1.22	3.14–3.48 (for C_α), 3.38–3.63 (for C_β)	170.8–178.1		[66]
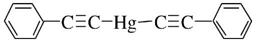	3.75–4.25		2.00	1.19	3.33–3.44 (for C_α), 3.64–3.77 (for C_β)	174.3–178.6		[66]
$PhHg(C{\equiv}CCF_3)$			2.029	1.192	3.582 (for C_α), 3.910 (for C_β)	175.3	170.2	[71]
$FcHg(C{\equiv}CCF_3)$	4.0882		2.050	1.183	3.359 (for C_α), 3.487 (for C_β)	179.4	178.1	[71]
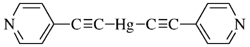			2.02	1.17–1.19		172	166–171	[74]
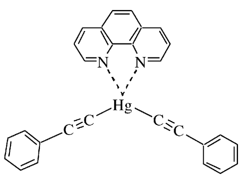			2.03, 2.05	1.17		165.6	170–173	[76]
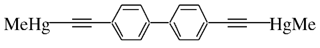	3.833–4.506	2.063	2.031	1.233		178.7	170.8	[78]
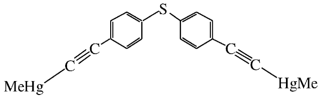	4.130–4.147	2.044, 2.065	2.011, 2.045	1.191, 1.211		176.9, 177.2	172.0, 176.6	[83]
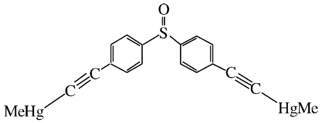	3.671–4.202	2.023, 2.106	2.031, 2.036	1.193, 1.200		177.3, 177.8	174.7, 178.9	[83]
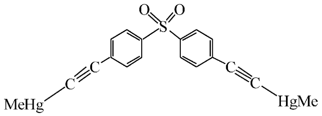	3.621–4.343	2.043, 2.065	2.043, 2.052	1.193, 1.199		176.8, 179.5	175.5, 175.6	[83]
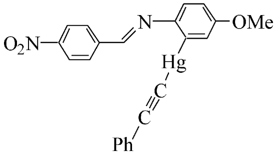	3.959		2.016	1.196	3.398 (for C_α), 3.783 (for C_β)	178.3	170.2	[84]
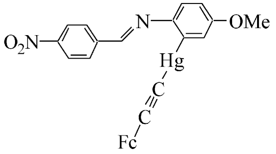	4.21		2.02	1.18	3.41 (for C_α), 3.57 (for C_β)	179.3	173	[84]

Table 1 (*Continued*)

Complex	Hg···Hg (Å)	Hg–CH_3 (Å)	Hg–C≡ (Å)	C≡C (Å)	Hg–C≡C(η^2) (Å)	C–Hg–C (°)	Hg–C≡C (°)	References
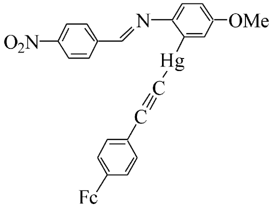			2.023	1.18		177.6	177.7	[84]
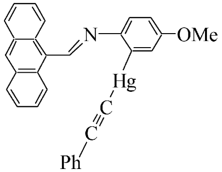			2.05	1.16		179.0	178.5	[84]
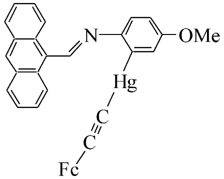			2.045	1.169		178.8	175.5	[84]
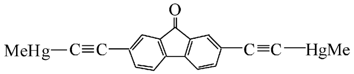		2.06	2.03, 2.05	1.16, 1.19		176.5, 178.0	170, 171	[92]
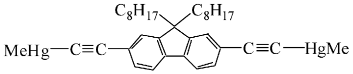	3.738–4.183	2.059, 2.080	2.044, 2.045	1.19, 1.21		177.6, 177.7	176.1, 176.8	[102]
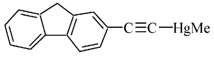	3.990–4.290	2.015, 2.057	2.048, 2.064	1.166, 1.176		173.4, 175.4	166.8, 167.3	[109]
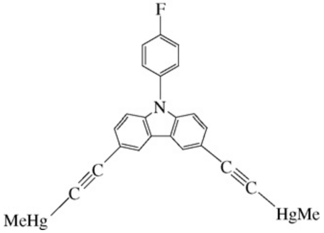	3.963–4.484	2.06	2.03	1.21		176.6	173.4	[112]
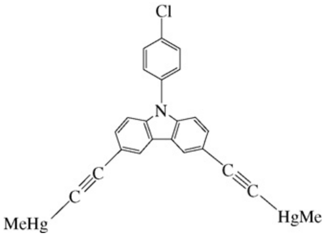	3.866–4.441	2.03, 2.06	2.02, 2.07	1.19, 1.27		176.1, 179.0	171, 173	[113]

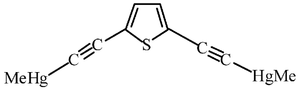	3.777–3.935	2.052, 2.065	2.036, 2.042	1.196, 1.202		176.0, 177.8	174.2, 175.4	[115]
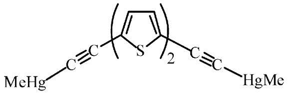	3.851	2.06, 2.07	2.02, 2.05	1.22, 1.26		174.3, 175.4	166	[115]
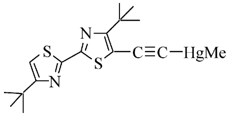		2.077	2.034	1.184		179.6	179.5	[116]
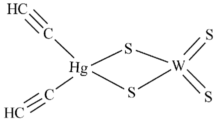			2.00, 2.05	1.15, 1.16		147	172, 177	[117]
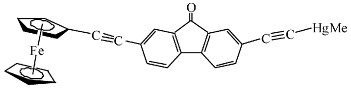		2.041	2.050	1.16		179.0	178.5	[118]
$[Hg(C{\equiv}CPh)_2Cu_2(MeCN)_4]\ [PF_6]_2$	8.48		2.006	1.246		180.0	165.7	[121]
$\{[Hg(C{\equiv}CTol)_2Ag][BF_4]\}_n$	5.66		2.00, 2.02	1.22		177.9	173	[121]
$[Hg(C{\equiv}CPh)_2Ag_2(bipy)_2][BF_4]_2$	9.53		2.017	1.209		180.0	167.8	[121]
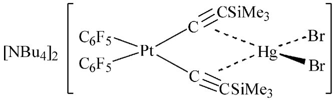				1.19, 1.21	2.41, 2.46 (for C_α), 2.57, 2.64 (for C_β)			[123]
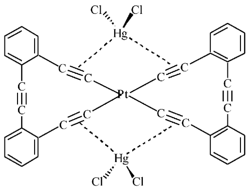					2.51, 2.55 (for C_α), 2.70, 2.77 (for C_β)			[125]
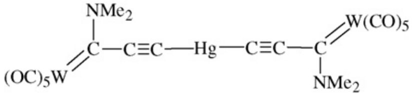			1.994	1.20		180.0	175	[127]
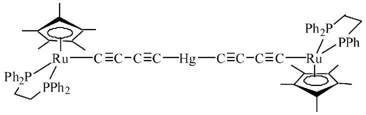			1.981	1.217, 1.224		180.0	166.5	[130]

the crystal structure reveals that a loose 1D polymeric aggregate is formed for the first time through a combination of weak intermolecular Hg· · ·Hg and Hg· · ·η^2-C≡C interactions to afford an infinite zigzag chain of Hg atoms supported by acetylide linkages. Interestingly, there is a strong tendency for the molecules in **22** to aggregate together and the lattice structure of **22** is highlighted by the extensive non-covalent Hg· · ·Hg and Hg· · ·η^2-C≡C interactive vectors, which links up the molecular units to result in a loose polymeric structure. Such polymeric aggregate shows a zigzag 1D chain of Hg atoms with an Hg· · ·Hg interaction distance of ca. 3.959 Å between adjacent molecules and the average Hg–Hg–Hg bond angle is 135.9° (Fig. 15). For comparison, crystals of $Hg_3(AlCl_4)_2$ [143] and Hg_3AsF_6 [144] also contain polymeric zigzag mercury chains in their lattices. A similar chain-like structure supported by alkynyl ligands is also found for silver(I) in $[(Me_3P)AgC{\equiv}CR]_\infty$ (R = Ph, $SiMe_3$) [145]. The intermolecular distances from the Hg atom to C_α(Hg(1)· · ·C(15)) and C_β(Hg(1)· · ·C(16)) are 3.398 and 3.783 Å, respectively, which compare well with the values quoted for **1h** and **1i** [66] but are significantly longer than the intramolecular distances found in **88** and **91**. Examination of the crystal packing diagram for **62** reveals the involvement of ligand-unsupported mercurophilicity in its structure with various weak intermolecular non-covalent Hg· · ·Hg interactions (3.963–4.484 Å). For **63**, the whole lattice structure is also supported and stabilized by extensive non-covalent d^{10}–d^{10}

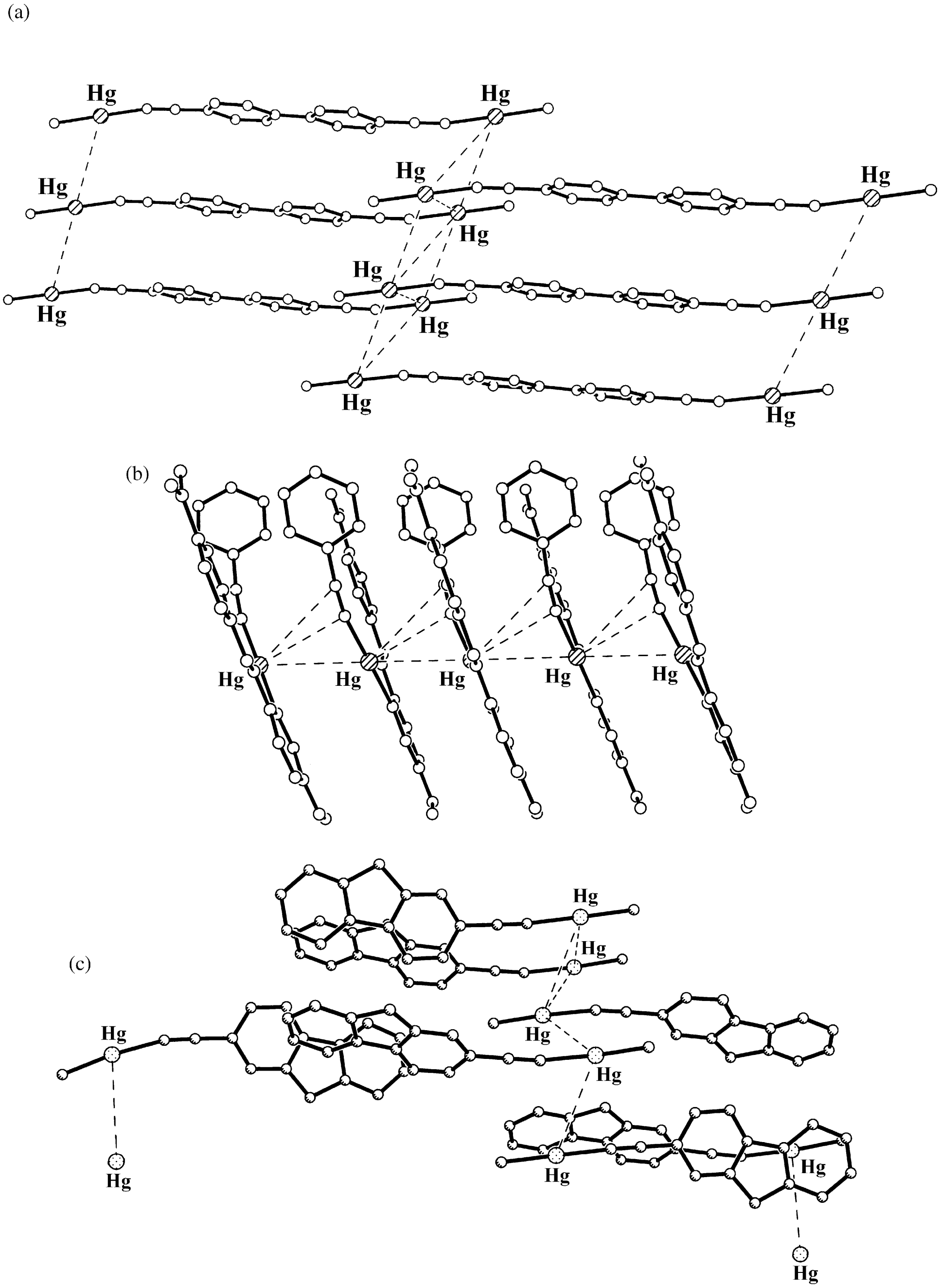

Fig. 15. Views of the packing diagrams showing the mercurophilic interactions for: (a) **9** [78], (b) **22** [84], (c) **45** [109], (d) **62** [112], (e) **68** [115], and (f) **69** [115].

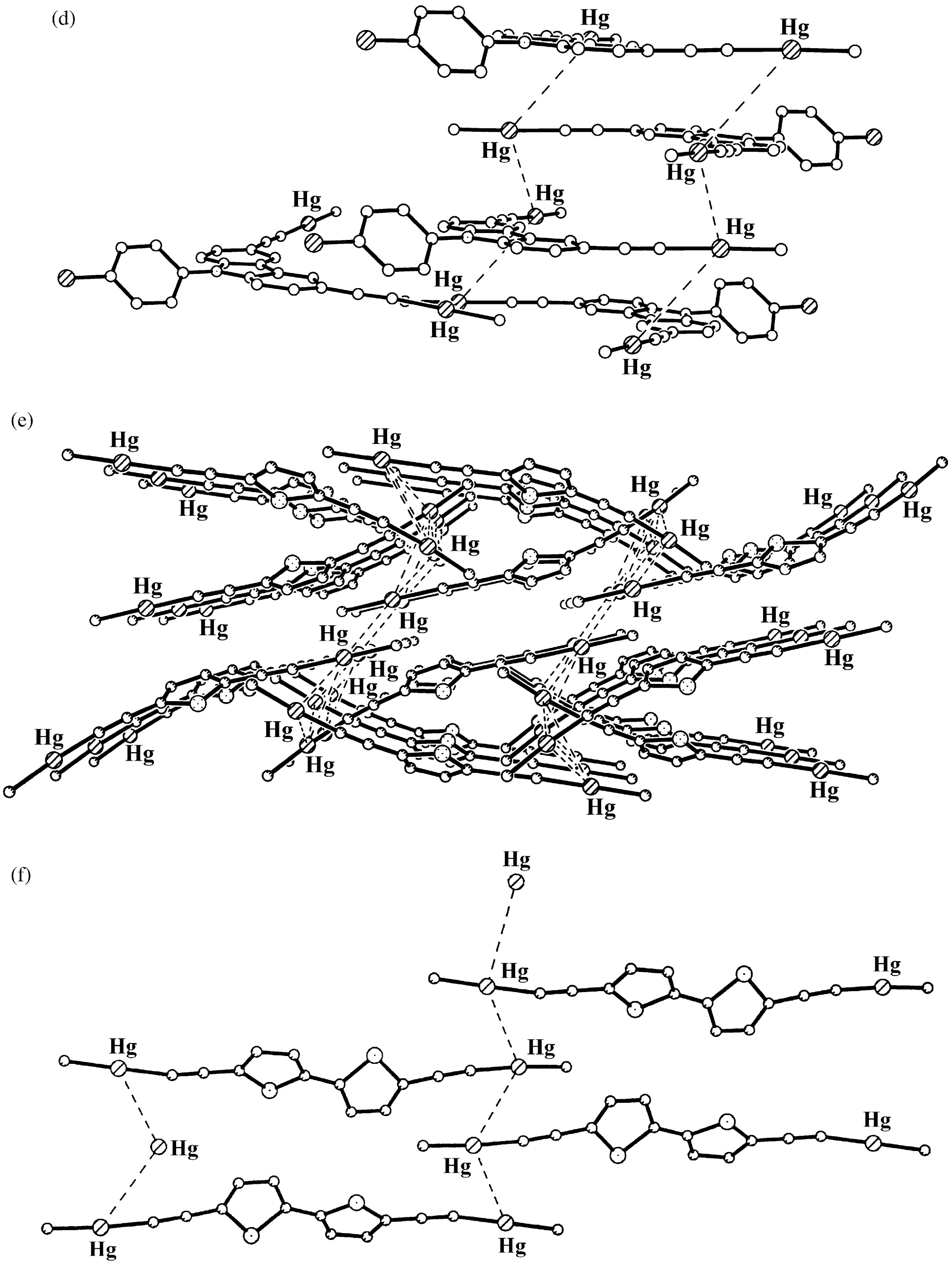

Fig. 15. (*Continued*).

Hg· · ·Hg interactive vectors (ca. 3.866 and 4.441 Å). As shown in Fig. 15, the lattice is characterized by infinite zig-zag chains of Hg atoms between adjacent molecules. This structure is unique in that no apparent weak Hg· · ·η^2-C≡C interactions are observed which are commonly the driving force for the solid-state aggregation to be observed in alkynyl complexes of Cu(I) and Ag(I).

5. Potential analytical applications

Mercury is a heavy metal that plays a key role in environmental politics due to its high general and specific neurotoxicity [146,147]. Mercury contamination is widespread via a variety of natural and anthropogenic sources including solid-waste incineration and the large-scale combustion of fossil fuels. Long-term and increasing interest in the speciation of inorganic mercury, Hg^{2+}, and monomethylmercury cation, $(MeHg)^+$, in environmental and biological samples has resulted in a large number of published analytical methods [148–152]. As a consequence, the detection and determination of mercury is of great scientific, medical and economic concern which continues the stimulation of the development of new techniques of analysis. The mercury ion has a rich but rather simple coordination chemistry. This simplicity forms the basis for its use as a highly selective reagent in various biological systems [153]. Thiol ligands were largely employed initially since thiolate ions are known to form very strong bonds with $(MeHg)^+$ to afford thermodynamically stable

MeHg-thiol complexes [154]. Attention has also been paid on the use of sodium tetraethylborate as a very successful alkylating reagent in the formation of alkylated organometallic derivatives for chromatographic analysis [155]. Alternatively, derivatization procedures which convert Hg^{2+} and $(MeHg)^+$ species into organometallic acetylide derivatives are becoming popular and rely on a simple analytical protocol using common commercial instrumentation. Following alkyne derivatization and solvent extraction, the resulting mercury alkynyls can be separated and analyzed by GC and HPLC techniques. Generally, HPLC has an advantage over GC since it is not necessary to form volatile derivatives in the former case [156,157].

Exploitation of alkyne-mercury coordination chemistry in environmental studies was well known for mercury speciation in water. A range of alkyne ligands have been used by several groups for alkynylating complexation with mercuric ion, in which an aromatic functional group is photophysically active in the UV–vis region, and, as a further design advantage, the synthesis was straightforward and required only simple routine chemistry [109,116,156–158]. Here, conversion of Hg(II) ion dissolved in water into stable mononuclear Hg(II) acetylides takes place smoothly in satisfactory yield under alkaline conditions by stirring the aqueous solution of Hg(II) salts with monosubstituted alkynes at room temperature, by analogy to the classical reactivity of Hg(II) species towards acetylenes. Among these, Trombini et al. have utilized phenylacetylene as the ligand precursor in the development of a novel procedure for inorganic Hg^{2+} and $(MeHg)^+$ species for HPLC analysis. The rate constants of the reactions of Hg^{2+} and $(MeHg)^+$ species in water with phenylacetylene are very high since the reaction occurs in 40 min at the ppb (10^{-9}) level under heterogeneous conditions [156,157]. The effect of interfering metal ions and the validity of the method for environmental samples such as seawater were investigated in detail. Recently, the same research team exploited another mercuration reaction starting from 10-(3-trimethylsilyl-2-propynyl)-9-(10*H*)-acridone to give **3** which seems promising in the $(MeHg)^+$ recognition and quantitation in biological samples such as tuna fish tissues [158]. This method for $(MeHg)^+$ determination competes well in terms of efficiency with the routinely used gas chromatography-electron capture detector (GC-ECD) techniques, and in terms of practicality with the widely used ethylation-based protocols which require sample pretreatment with $NaBEt_4$ under strictly controlled conditions, followed by GC–pyrolysis–CVAFS (CVAFS, cold vapor atomic fluorescence spectroscopy). Importantly, the results are practically unaffected by other interfering species such as AgBr and CuBr.

In the context of these important areas, we choose **51** and **52** as illustrative examples and their unique photophysical features appear to be appropriate for straightforward analytical detection. $HgCl_2$ dissolved in alkaline aqueous solution could be complexed by various monoethynylfluorene ligands and converted into mercury acetylides in high derivatization yields which can easily be extracted into organic solvents. This was clearly confirmed by preliminary HPLC measurements [109]. Dose–response curves for **51** and **52** were measured, and a good proportionality was observed between the amount of analyte injected and peak areas. Calibration graphs based on peak areas are shown in Fig. 16, and are linear over 12.5–100.0 mg/L for **51** with a correlation coefficient of 0.9999 and 2.5–196.0 mg/L for **52** with a correlation coefficient of 0.9996. The excellent fit and linearity indicates that this method is suitable for quantitative analysis. The detection limit, expressed as the absolute amount of analyte injected to give a signal three times higher than the signal noise, was found to be ~0.5 ng injected Hg for **51** and **52** in each case.

Tables 2 and 3 collect the calculated concentrations of Hg(II) ion of the working solutions in deionized water and seawater samples, respectively, and the corresponding percent recoveries. Our results show that the Hg(II) concentrations determined according to the proposed procedure match quite well the expected values (recovery ≥90% at 2.5 ppm with derivatization time of 2 h) and reflect the nearly quantitative yield of the reaction and extraction step in several cases (entries 6 and 7 in Table 2). Short derivatization time (ca. 0.5 h in entries 4 and 5 in Table 2) still afforded a reasonably good percent recovery (>67%) for **51**. Likewise, the results are also very good for **52** with recovery >95% at 10 ppm.

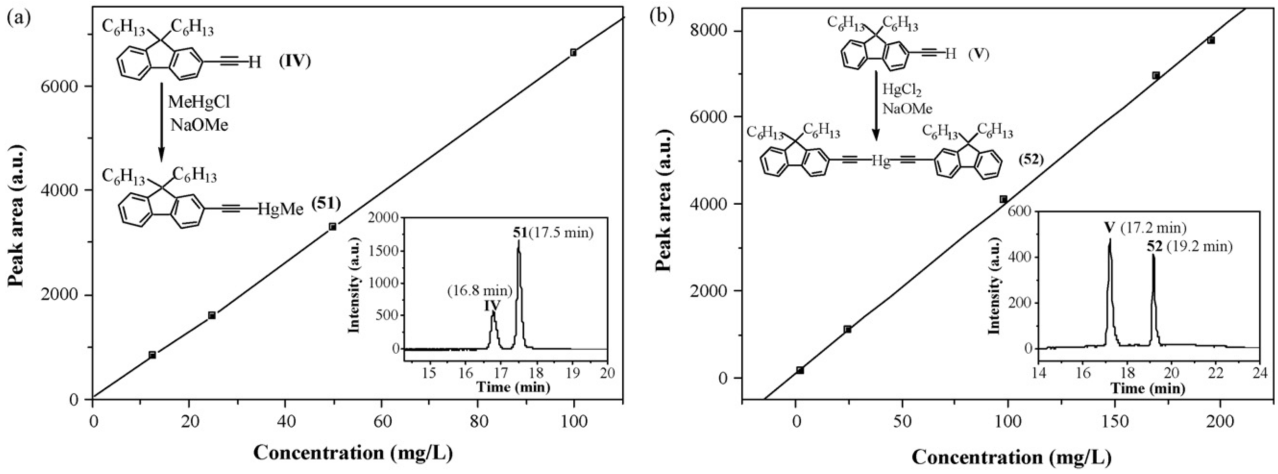

Fig. 16. Calibration graphs and the chromatograms (the inset) for analytes (a) **51** and (b) **52** [109].

Table 2
Determination of inorganic mercury in D.I. water as **51** in THF[a]

Hg concentration (mg/L)	Found Hg concentration (mg/L)	Recovery (%)
1.710 ± 0.006	1.390 ± 0.005	81.23
2.402 ± 0.005	2.147 ± 0.008	89.30
3.043 ± 0.005	2.705 ± 0.007	88.90
2.357 ± 0.005[b]	1.600 ± 0.009	67.89
3.121 ± 0.007[b]	2.270 ± 0.005	72.73
4.035 ± 0.006	3.743 ± 0.005	92.76
5.629 ± 0.007	5.184 ± 0.009	92.10

[a] Working solution, 50 mL; [NaOH] = 0.20 M; [NaCl] = 0.25 M. All experiments refer to three replicate analyses of working solution.

[b] Derivatization time is ca. 0.5 h.

Analysis of seawater samples spiked with $HgCl_2$ using this methodology has been probed with much success. It seems that the percent recovery of **51** in seawater condition is lower than that in deionized water condition. It may be due to the presence of some interfering ions, such as other metal ions, in the sea water to affect the formation of the Hg(II) complexes. Presumably, colloidal alkaline-earth hydroxides formed in the required alkaline conditions and/or natural organic complexing reagents could affect the derivatization and/or the extraction step. The results tabulated in Table 3 are reasonably attractive, with the recoveries of Hg(II) species being close to 44% at the concentration of 2.5 ppm and even 63% at 5 ppm level. The performance appears to be better than those using phenylacetylene as the complexing agent. Even though the procedure can be further improved, these preliminary results obtained in seawater are quite promising for future materials and methodology design. The same strategy can also be applied to other organomercurial systems with bithiazole chromophores for the simultaneous determination of inorganic Hg^{2+} and organic $(MeHg)^+$ in aqueous solutions (vide supra) [116]. We believe that such studies represent a promising starting point for the development of a rapid and sensitive method for the analysis of mercuric ion in an aqueous medium.

Table 3
Determination of inorganic mercury in seawater as **51** in THF[a]

Hg concentration (mg/L)	Found Hg concentration (mg/L)	Recovery (%)
2.560 ± 0.005	1.135 ± 0.009	44.3
3.723 ± 0.007	1.866 ± 0.010	50.1
4.005 ± 0.005	2.331 ± 0.008	58.2
5.012 ± 0.006	3.172 ± 0.010	63.3

[a] Working solution, 50 mL; [NaOH] = 0.20 M; [NaCl] = 0.25 M. All experiments refer to three replicate analyses of working solution.

Bunz and co-workers have demonstrated interesting sensor applications of some polar PPEs **111–113** in which two of them (**112** and **113**) carry β-glucopyranose substituents. Depending on the linker used between the glycol units and the polymeric backbone, the fluorescence of these PPEs can be quenched by Hg^{2+} ions to a varying degree [159]. It was anticipated that the unusually high acidity of Hg^{2+} ion leads to a higher than expected binding constant to alcohol OH moieties in which the authors postulate a hexacoordination of Hg^{2+} ion that is surrounded by three glucose molecules. The same authors further reported that proteins can effectively modulate the sensor properties of **114** and **115** through electrostatic complex formation. The detection of Hg^{2+} by **114**-papain reveals clearly that specific properties of proteins strongly influence the emissive behavior of conjugated polymers [160].

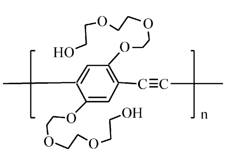

111

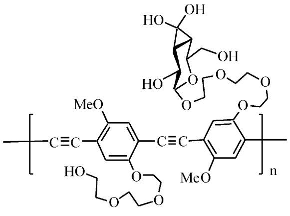

112

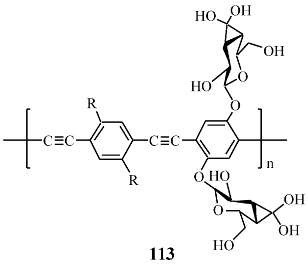

113

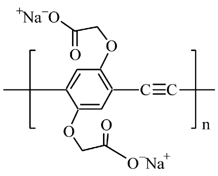

114

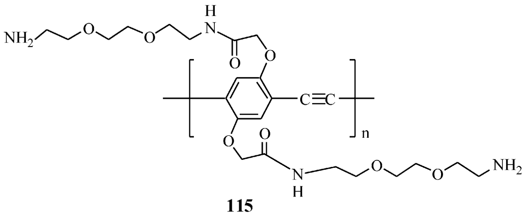

115

6. Concluding remarks and outlook

Taking into account the affinity that mercuric ions display for organic alkynes, the chemistry of group 12 metal-alkynyls, especially the d^{10} mercury(II)-alkynyl compounds, however, has not been so thoroughly investigated. Indeed, mono-, di- and polyalkynyl mercury complexes were demonstrated to be useful in the analysis of toxic Hg(II) species and to be good structural units for the synthesis of luminescent metallopolymers and supramolecular aggregates. Despite their inherent toxicity, organomercurials are among one of the most widely studied of organometallic compounds, in part because of their synthetic utility as convenient and efficient organo-transfer reagents, and more recently for their potential to exhibit closed-shell mercurophilic interactions in the solid state. Being a relatively cheap chemical for mercury metal, compounds derived from it also hold a recent fascination for practitioners in the area of conjugated organic polymers, analytical and organometallic chemists, and workers in the field of synthetic metal-containing polymers.

Over the past few years, impressive progress has been made in the area of luminescent organomercury acetylide complexes and polymers, in which such organometallic building blocks adopt a linear two-coordinate configuration to provide a rigid-rod framework. Solubility issue may be alleviated by appropriate functionalization of the organic groups. Harvesting of organic triplet emissions harnessed through the strong heavy-atom effects of mercury metal was comprehensively probed in distinct molecular and polymeric metallized systems. This provides us a unique opportunity to study the relationship between triplet energy and the rate of non-radiative decay for this class of conjugated materials. If they can be further activated to be multifunctional, the work has great potential to excel in optoelectronics that demand low manufacturing cost and light energy harvesting from the T_1 state. The development of such analytical protocols for the rapid and cheap control of environmental pollutants represents a key goal of analytical green chemistry that certainly deserves further examination. In the area of analytical chemistry, future work will be focused on the effect of other interfering agents and matrix components in the Hg(II) speciation. Our scope of the procedure may also be evaluated by applying the methodology to other environmental samples such as tissues and sediments collected in a severely contaminated area. All in all, continuing research study and refinement along this direction could broaden the scope to other metallo organic triplet-emitting and chemosensing systems.

Acknowledgements

The author gratefully acknowledges financial support from the Research Grants Council of the Hong Kong SAR (HKBU 2022/03P) and the Hong Kong Baptist University. He is also indebted to all his postgraduate students and postdoctoral research associates for their contribution cited in the references of this review. Thanks are also due to the technical assistance from Ms. Cheuk-Lam Ho and Mr. Xingzhu Wang.

References

[1] Y. Fujikura, K. Sonogashira, N. Hagihara, Chem. Lett. (1975) 1067.
[2] K. Sonogashira, S. Takahashi, N. Hagihara, Macromolecules 10 (1977) 879.
[3] S. Takahashi, M. Kariya, T. Yatake, K. Sonogashira, N. Hagihara, Macromolecules 11 (1978) 1063.
[4] K. Sonogashira, S. Kataoka, S. Takahashi, N. Hagihara, J. Organomet. Chem. 160 (1978) 319.
[5] R.H. Friend, R.W. Gymer, A.B. Holmes, J.H. Burroughes, R.N. Marks, C. Taliani, D.D.C. Bradley, D.A. Dos Santos, J.L. Bredas, M. Lögdlund, W.R. Salaneck, Nature (London) 397 (1999) 121.
[6] J.S. Wilson, A.S. Dhoot, A.J.A.B. Seeley, M.S. Khan, A. Köhler, R.H. Friend, Nature (London) 413 (2001) 828.
[7] A. Köhler, J.S. Wilson, R.H. Friend, Adv. Mater. 14 (2002) 701.
[8] C. Adachi, M.A. Baldo, M.E. Thompson, S.R. Forrest, J. Appl. Lett. 90 (2001) 5048.
[9] J.M. Lupton, A. Pogantsch, T. Piok, E.J.W. List, S. Patil, U. Scherf, Phys. Rev. Lett. 89 (2002) 167401.
[10] R.C. Evans, P. Douglas, C.J. Winscom, Coord. Chem. Rev. 250 (2006) 2093.
[11] X. Gong, J.C. Ostrowski, G.C. Bazan, D. Moses, A.J. Heeger, M.S. Liu, A.K.-Y. Jen, Adv. Mater. 15 (2003) 45.
[12] A.S. Dhoot, N.C. Greenham, Adv. Mater. 14 (2002) 1834.
[13] I. Manners, Synthetic Metal-Containing Polymers, Wiley-VCH, Weinheim, 2004, p. 153 (Chapter 5).
[14] P. Nguyen, P. Gómez-Elipe, I. Manners, Chem. Rev. 99 (1999) 1515.
[15] I. Manners, Angew. Chem. Int. Ed. Engl. 35 (1996) 1602.
[16] A.S. Abd-El-Aziz, Macromol. Rapid Commun. 23 (2002) 995.
[17] R.P. Kingsborough, T.M. Swager, Prog. Inorg. Chem. 48 (1999) 123.
[18] N.J. Long, C.K. Williams, Angew. Chem. Int. Ed. 42 (2003) 2586.
[19] W.-Y. Wong, J. Inorg. Organomet. Polym. Mater. 15 (2005) 197.
[20] W.-Y. Wong, Comment Inorg. Chem. 26 (2005) 39.
[21] W.-Y. Wong, C.-L. Ho, Coord. Chem. Rev. 250 (2006) 2627.
[22] I. Manners, Science 294 (2001) 1664.
[23] R.J. Puddephatt, Chem. Commun. (1998) 1055.
[24] R.J. Puddephatt, Coord. Chem. Rev. 216–217 (2001) 313.
[25] V.W.W. Yam, K.K.W. Lo, K.M.C. Wong, J. Organomet. Chem. 578 (1999) 3.
[26] H.Y. Chao, W. Lu, Y. Li, M.C.W. Chan, C.M. Che, K.K. Cheung, N. Zhu, J. Am. Chem. Soc. 124 (2002) 14696.
[27] W. Lu, H.-F. Xiang, N. Zhu, C.-M. Che, Organometallics 21 (2002) 2343.
[28] C.-M. Che, H.-Y. Chao, V.M. Mskowski, Y. Li, K.-K. Cheung, J. Am. Chem. Soc. 123 (2001) 4985.
[29] B. Ahrens, K.-H. Choi, M.S. Khan, P. Li, P.R. Raithby, P.J. Wilson, W.-Y. Wong, Cryst. Eng. Commun. 4 (2002) 405.
[30] W. Lu, N. Zhu, C.-M. Che, J. Organomet. Chem. 670 (2003) 11.
[31] J. Vicente, M.T. Chicote, M.D. Abrisqueta, M.M. Alvarez-Falcón, J. Organomet. Chem. 663 (2002) 40.
[32] J. Vicente, M.-T. Chicote, M.M. Alvarez-Falcón, Organometallics 23 (2004) 5707.
[33] J. Vicente, M.-T. Chicote, M.M. Alvarez-Falcón, Organometallics 24 (2005) 2764.
[34] H. Schmidbaur, Gold Bull. 23 (1990) 11.
[35] H. Schmidbaur, Chem. Soc. Rev. 24 (1995) 391.
[36] B.C. Hollatz, A. Schier, H. Schmidbaur, Inorg. Chem. 38 (1999) 3978.
[37] C. Hollatz, A. Schier, H. Schmidbaur, J. Am. Chem. Soc. 119 (1997) 8115.
[38] C. King, J.C. Wang, M.N.I. Kham, J.P. Fackler Jr., Inorg. Chem. 28 (1989) 2145.
[39] M.J. Irwin, J.J. Vittal, R.J. Puddephatt, Organometallics 16 (1997) 3541.
[40] W.J. Hunks, M.A. MacDonals, M.C. Jennings, R.J. Puddephatt, Organometallics 19 (2000) 5063.
[41] J.R. Johnson, W.L. McEwan, J. Am. Chem. Soc. 48 (1926) 469.
[42] A.F. Hill, M.C.J. Harris, R.P. Melling, Polyhedron 11 (1992) 781.
[43] X.L.R. Fontaine, S.J. Higgins, C.R. Langrick, B.L. Shaw, J. Chem. Soc., Dalton Trans. (1987) 777.
[44] R.J. Cross, J. Gemmill, J. Chem. Soc., Dalton Trans. (1984) 199.
[45] Y.-K. Au, W.-T. Wong, J. Chem. Soc., Dalton Trans. (1995) 1389.
[46] F.A. Cotton, G. Wilkinson, C.A. Murillo, M. Bochmann, Advanced Inorganic Chemistry, 6th ed., Wiley, 1999.
[47] J.S. Casas, M.S. Garcia-Tasende, J. Sordo, Coord. Chem. Rev. 193–195 (1999) 283.
[48] R. Nast, Coord. Chem. Rev. 47 (1982) 89.
[49] C. Furlani, M.N. Piancastelli, C. Cauletti, F. Faticanti, G. Ortaggi, J. Electron. Spectrosc. Relat. Phenom. 22 (1981) 309.
[50] J. Manna, K.D. John, M.D. Hopkins, Adv. Organomet. Chem. 38 (1995) 79.
[51] M.L.H. Green, in: G.E. Coates, H.M.L. Green, K. Wade (Eds.), Organometallic Compounds, 3rd ed., Methuen, London, 1968.
[52] M.I. Bruce, R. Clark, J. Howard, P. Woodward, J. Organomet. Chem. 42 (1972) C107.
[53] O.M. Abu Salah, M.I. Bruce, J. Chem. Soc., Dalton Trans. (1974) 2302.
[54] J.P. Collman, J.W. Kang, J. Am. Chem. Soc. 89 (1967) 844.
[55] K. Takagi, N. Hayama, T. Okamoto, Y. Sakakibara, S. Oka, Bull. Chem. Soc. Jpn. 50 (1977) 2741.
[56] A.F. Hill, J.D.E.T. Wilton-Ely, Organometallics 16 (1997) 4517.

[57] S.J. Higgins, R. Taylor, B.L. Shaw, J. Organomet. Chem. 325 (1987) 285.
[58] B.F.G. Johnson, J. Lewis, P.R. Raithby, D.A. Wilkinson, J. Organomet. Chem. 408 (1991) C9.
[59] E.M. Cano, M.A. Santos, R.L. Ballester, Anal. Quim. 73 (1977) 1051.
[60] D. Seyferth, D.P. Ruschke, W.M. Davis, M. Cowie, A.D. Hunter, Organometallics 13 (1994) 3834.
[61] E.A. Dikusar, V.I. Potkin, E.V. Vashkevich, N.G. Kozlov, R.V. Kaberdin, Russian J. Gen. Chem. 74 (2004) 578.
[62] E.A. Dikusar, N.G. Kozlov, S.S. Koval'skaya, L.A. Popova, K.L. Moiseichuk, Russian J. Gen. Chem. 71 (2001) 290.
[63] A. Sebald, B. Wrackmeyer, Spectrochim. Acta 38A (1982) 163.
[64] Y. Imai, F. Watari, K. Aida, Spectrochim. Acta 36A (1980) 233.
[65] Y. Imai, K. Aida, Bull. Chem. Soc. Jpn. 52 (1979) 2875.
[66] S.J. Faville, W. Henderson, T.J. Mathieson, B.K. Nicholson, J. Organomet. Chem. 580 (1999) 363.
[67] R.J. Cross, M.F. Davidson, J. Chem. Soc., Dalton Trans. (1986) 1987.
[68] C.R. Langrick, D.M. McEwan, P.G. Pringle, B.L. Shaw, J. Chem. Soc., Dalton Trans. (1983) 2487.
[69] C.M. Forsyth, G.B. Deacon, L.D. Field, C. Jones, P.C. Junk, D.L. Kay, A.F. Masters, A.F. Richards, Chem. Commun. (2006) 1003.
[70] A.K. Brisdon, I.R. Crossley, Chem. Commun. (2002) 2420.
[71] A.K. Brisdon, I.R. Crossley, R.G. Pritchard, Organometallics 24 (2005) 5487.
[72] R.D. Dewhurst, A.F. Hill, M.K. Smith, Organometallics 25 (2006) 2388.
[73] F. Bolletta, D. Fabbri, M. Lombardo, L. Prodi, C. Trombini, N. Zaccheroni, Organometallics 15 (1996) 2415.
[74] B.F. Hoskins, R. Robson, E.E. Sutherland, J. Organomet. Chem. 515 (1996) 259.
[75] M. Ferrer, L. Rodriguez, O. Rossell, F. Pina, J.C. Lima, M.F. Bardia, X. Solans, J. Organomet. Chem. 678 (2003) 82.
[76] E. Gutiérrez-Puebla, A. Vegas, Acta Cryst. B34 (1978) 3382.
[77] E. Gutiérrez-Puebla, A. Vegas, S. Garcia-Blanco, Cryst. Struct. Commun. 8 (1979) 861.
[78] L. Liu, S.-Y. Poon, W.-Y. Wong, J. Organomet. Chem. 690 (2005) 5036.
[79] G. Frapper, M. Kertesz, Inorg. Chem. 32 (1993) 732.
[80] T.-J. Taylor, F.-P. Gabbaï, Organometallics 25 (2006) 2143.
[81] L. Liu, W.-Y. Wong, C.-L. Ho, Aust. J. Chem. 59 (2006) 1.
[82] L. Liu, M.-X. Li, W.-Y. Wong, Aust. J. Chem. 58 (2005) 799.
[83] S.-Y. Poon, W.-Y. Wong, K.-W. Cheah, J.-X. Shi, Chem. Eur. J. 12 (2006) 2550.
[84] W.-Y. Wong, G.-L. Lu, L. Liu, J.-X. Shi, Z. Lin, Eur. J. Inorg. Chem. (2004) 2066.
[85] W.-Y. Wong, Coord. Chem. Rev. 249 (2005) 971.
[86] D. Neher, Macromol. Rapid Commun. 22 (2001) 1365.
[87] B. Tsuie, J.L. Reddinger, G.A. Sotzing, J. Soloducho, A.R. Katritzky, J.R. Reynolds, J. Mater. Chem. 9 (1999) 2189.
[88] K.-T. Wong, Y.-Y. Chien, R.-T. Chen, C.-F. Wang, Y.-T. Lin, H.-H. Chiang, P.-Y. Hsieh, C.-C. Wu, C.-H. Chou, Y.O. Su, J. Am. Chem. Soc. 124 (2002) 11576.
[89] W.-L. Yu, J. Pei, W. Huang, A.J. Heeger, Adv. Mater. 12 (2000) 828.
[90] S. Setayesh, A.C. Grimsdale, T. Weil, V. Enkelmann, K. Müllen, F. Meghdadi, E.J.W. List, G. Leising, J. Am. Chem. Soc. 123 (2001) 946.
[91] W.-Y. Wong, G.-J. Zhou, X.-M. Yu, H.-S. Kwok, B. Tang, Adv. Funct. Mater. 16 (2006) 838.
[92] W.-Y. Wong, K.-H. Choi, G.-L. Lu, J.-X. Shi, P.-Y. Lai, S.-M. Chan, Organometallics 20 (2001) 5446.
[93] L. Liu, Z.-X. Chen, S.-Z. Liu, W.-Y. Wong, Acta Chim. Sin. 64 (2006) 884.
[94] W.-Y. Wong, G.-L. Lu, K.-H. Choi, J.-X. Shi, Macromolecules 25 (2002) 3506.
[95] P.K.H. Ho, J.S. Kim, J.H. Burroughes, H. Becker, S.F.Y. Li, T.M. Brown, F. Cacialli, R.H. Friend, Nature (London) 404 (2000) 481.
[96] Y. Cao, I.D. Parker, G. Yu, C. Zhang, A.J. Heeger, Nature (London) 397 (1999) 414.
[97] V. Cleave, G. Yahioglu, P. Le Bamy, R.H. Friend, N. Tessler, Adv. Mater. 11 (1999) 285.
[98] M.A. Baldo, D.F. O'Brien, Y. You, A. Shoustikov, S. Sibley, M.E. Thompson, S.R. Forrest, Nature (London) 395 (1998) 151.
[99] M.A. Baldo, M.E. Thompson, S.R. Forrest, Nature (London) 403 (2000) 750.
[100] M. Pope, C.E. Swenberg, Electronic Processes in Organic Crystals and Polymers, 2nd ed., Oxford Science Publications, Oxford, 1999.
[101] J.S. Wilson, N. Chawdhury, M.R.A. Al-Mandhary, M. Younus, M.S. Khan, P.R. Raithby, A. Köhler, R.H. Friend, J. Am. Chem. Soc. 123 (2001) 9412.
[102] W.-Y. Wong, L. Liu, J.-X. Shi, Angew. Chem. Int. Ed. 42 (2003) 4064.
[103] U.H.F. Bunz, Chem. Rev. 100 (2000) 1605.
[104] G.-J. Zhou, W.-Y. Wong, Z. Lin, C. Ye, Angew. Chem. Int. Ed. 45 (2006) 6189.
[105] A. Köhler, J.S. Wilson, R.H. Friend, M.K. Al-Suti, M.S. Khan, A. Gerhard, H. Bässler, J. Chem. Phys. 116 (2002) 9457.
[106] A.P. Monkman, H.D. Burrows, L.J. Hartwell, L.E. Horsburgh, I. Hamblett, S. Navaratnam, Phys. Rev. Lett. 86 (2001) 1358.
[107] Y.V. Romanovskii, A. Gerhard, B. Schweitzer, U. Scherf, R.I. Personov, H. Bässler, Phys. Rev. Lett. 84 (2000) 1027.
[108] Y. Liao, J.-K. Feng, L. Yang, A.-M. Ren, H.-X. Zhang, Organometallics 24 (2005) 385.
[109] L. Liu, W.-Y. Wong, Y.-W. Lam, W.-Y. Tam, Inorg. Chim. Acta 360 (2007) 109.
[110] L. Liu, W.-Y. Wong, S.-Y. Poon, J.-X. Shi, K.-W. Cheah, Z. Lin, Chem. Mater. 18 (2006) 1369.
[111] W.-Y. Wong, L. Liu, S.-Y. Poon, K.-H. Choi, K.-W. Cheah, J.-X. Shi, Macromolecules 37 (2004) 4496.
[112] L. Liu, W.-Y. Wong, J.-X. Shi, K.-W. Cheah, J. Polym. Sci. Part A: Polym. Chem. 44 (2006) 5588.
[113] L. Liu, W.-Y. Wong, J.-X. Shi, K.-W. Cheah, T.-H. Lee, L.-M. Leung, J. Organomet. Chem. 691 (2006) 4028.
[114] L. Liu, Z.-X. Chen, S.-Z. Liu, W.-Y. Wong, Chem. J. Chin. Univ. 27 (2006) 1282.
[115] W.-Y. Wong, K.-H. Choi, G.-L. Lu, Organometallics 21 (2002) 4475.
[116] L. Liu, Y.-W. Lam, W.-Y. Wong, J. Organomet. Chem. 691 (2006) 1092.
[117] I. Ghosh, R. Mshra, D. Poddar, A.-K. Mukherjee, M. Mukherjee, R. Bhattacharyya, Chem. Commun. (1996) 435.
[118] W.-Y. Wong, K.-Y. Ho, K.-H. Choi, J. Organomet. Chem. 670 (2003) 17.
[119] R.B. Bedford, A.F. Hill, A.R. Thompsett, A.J.P. White, D.J. Williams, Chem. Commun. (1996) 1059.
[120] R.D. Bedford, P.J. Dyson, A.F. Hill, A.G. Hulkes, C.J. Yates, Organometallics 17 (1998) 4117.
[121] D. Rais, D.M.P. Mingos, R. Vilar, A.J.P. White, D.J. Williams, Organometallics 19 (2000) 5209.
[122] D.M.P. Mingos, R. Vilar, D. Rais, J. Organomet. Chem. 641 (2002) 126.
[123] J.R. Berenguer, J. Forniés, E. Lalinde, A. Martin, M.T. Moreno, J. Chem. Soc., Dalton Trans. (1994) 3343.
[124] J. Fernández, J. Forniés, B. Gil, J. Gómez, E. Lalinde, M.T. Moreno, Organometallics 25 (2006) 2274.
[125] D. Zhang, D.B. McConville, C.A. Tessier, W.J. Youngs, Organometallics 16 (1997) 824.
[126] W. Frosch, A. del Villar, H. Lang, J. Organomet. Chem. 602 (2000) 91.
[127] C. Hartbaum, G. Roth, H. Fischer, Eur. J. Inorg. Chem. (1998) 191.
[128] C. Hartbaum, H. Fischer, J. Organomet. Chem. 578 (1999) 186.
[129] M.I. Bruce, M. Jevric, B.W. Skelton, M.E. Smith, A.H. White, N.N. Zaitseva, J. Organomet. Chem. 691 (2006) 361.
[130] M.I. Bruce, J.F. Halet, B.L. Guennic, B.W. Skelton, M.E. Smith, A.H. White, Inorg. Chim. Acta 350 (2003) 175.
[131] R.D. Dewhurst, A.F. Hill, A.C. Willis, Organometallics 24 (2005) 3043.
[132] G.-C. Guo, T.C.W. Mak, Angew. Chem. Int. Ed. Engl. 37 (1998) 3268.
[133] G.-C. Guo, G.-D. Zhou, Q.-G. Wang, T.C.W. Mak, Angew. Chem. Int. Ed. Engl. 37 (1998) 630.
[134] J.-P. Zhang, Y.-B. Wang, X.-C. Hunag, Y.-Y. Lin, X.-M. Chen, Chem. Eur. J. 11 (2005) 552.
[135] P. Pyykkö, Chem. Rev. 97 (1997) 597.
[136] K.R. Flower, V.J. Howard, S. Naguthney, R.G. Pritchard, J.E. Warren, A.T. McGown, Inorg. Chem. 41 (2002) 1907.
[137] S.S. Batsanov, J. Chem. Soc., Dalton Trans. (1998) 1541.
[138] A. Bondi, J. Phys. Chem. 68 (1964) 441.

[139] J. Bravo, J.S. Casas, Y.P. Mascarenhas, A. Sanchez, C.O.P. de Santos, J. Sordo, J. Chem. Soc. Chem. Commun. (1986) 1100.

[140] N.L. Pickett, O. Just, D.G. VanDerveer, W.S. Rees Jr., Acta Cryst. C56 (2000) 412.

[141] X. Wang, L. Andrews, Inorg. Chem. 43 (2004) 7146.

[142] U. Patel, H.B. Singh, G. Wolmershäuser, Angew. Chem. Int. Ed. 44 (2005) 1715.

[143] I.D. Brown, B.D. Cutforth, C.G. Davies, R.J. Gillespie, P.R. Ireland, J.E. Vekris, Can. J. Chem. 52 (1974) 791.

[144] R.D. Ellison, H.A. Levy, K.W. Fung, Inorg. Chem. 11 (1972) 833.

[145] C. Brasse, P.R. Raithby, M.-A. Rennie, C.A. Russell, A. Steiner, D.S. Wright, Organometallics 15 (1996) 639.

[146] M.J. Scoullos, G.H. Vonkeman, L. Thornton, Z. Makuch, Mercury, Cadmium, Lead: Handbook for Sustainable Heavy Metals Policy and Regulation (Environment & Policy, V.31), Kluwer Academic, 2001.

[147] J.E. Fergusson, The Heavy Elements: Chemistry, Environmental Impact and Health Effects, Pergamon Press, Oxford, 1991 (Part II).

[148] D.S. Lee, E. Nemitz, D. Fowler, R.D. Kingdon, Atm. Environ. 35 (2001) 5455.

[149] E.M. Nolan, S.J. Lippard, J. Mater. Chem. 15 (2005) 2778.

[150] M.K. Nazeeruddin, D.D. Censo, R. Humphry-Baker, M. Grätzel, Adv. Funct. Mater. 16 (2006) 189.

[151] E.M. Nolan, S.J. Lippard, J. Am. Chem. Soc. 125 (2003) 14270.

[152] R. Puk, J.H. Weber, Appl. Organomet. Chem. 8 (1994) 293.

[153] R.D. Wilken, J. Fresenius, Anal. Chem. 342 (1992) 795.

[154] D.L. Rabenstein, Acc. Chem. Res. 11 (1978) 100.

[155] S. Rapsomanikis, Analyst 119 (1994) 1429.

[156] D. Fabbri, C. Trombini, Chromatographia 39 (1994) 246.

[157] D. Fabbri, M. Lombardo, C. Trombini, I. Vassura, Appl. Organomet. Chem. 9 (1995) 713.

[158] M. Lombardo, I. Vassura, D. Fabbri, C. Trombini, J. Organomet. Chem. 690 (2005) 588.

[159] I.B. Kim, B. Erdogan, J.N. Wilson, U.H.F. Bunz, Chem. Eur. J. 10 (2004) 6247.

[160] I.B. Kim, U.H.F. Bunz, J. Am. Chem. Soc. 128 (2006) 2818.